Broad Band Solitons in a Periodic and Nonlinear Maxwell System

Dmitry E. Pelinovsky* Gideon Simpson† Michael I. Weinstein‡

June 21, 2011

Abstract

We consider the one-dimensional Maxwell equations with low contrast periodic linear refractive index and weak Kerr nonlinearity. In this context, wave packet initial conditions with a single carrier frequency excite infinitely many resonances. On large but finite time-scales, the coupled evolution of backward and forward waves is governed by nonlocal equations of resonant nonlinear geometrical optics. For the special class of solutions which are periodic in the fast phase, these equations are equivalent to an infinite system of nonlinear coupled mode equations, the so called *extended nonlinear coupled mode equations*, xNLCME. Numerical studies support the existence of long-lived spatially localized coherent structures, featuring a slowly varying envelope and a train of *carrier shocks*. Thus, it is natural to study the localized coherent structures of xNLCME.

In this paper we explore, by analytical, asymptotic and numerical methods, the existence and properties of spatially localized structures of the xNLCME system, which arises for a refractive index profile consisting of periodic array of Dirac delta functions.

We consider, in particular, the limit of small amplitude solutions with frequencies near a band-edge. In this case, stationary xNLCME is well-approximated by an infinite system of coupled, stationary, nonlinear Schrödinger equations, the *extended nonlinear Schrödinger system*, xNLS. We embed xNLS in a one-parameter family of equations, xNLS$^\epsilon$, which interpolates between infinitely many decoupled NLS equations ($\epsilon = 0$) and xNLS ($\epsilon = 1$). Using bifurcation methods we show existence of solutions for a range of $\epsilon \in (-\epsilon_0, \epsilon_0)$ and, by a numerical continuation method, establish the continuation of certain branches all the way to $\epsilon = 1$. Finally, we perform time-dependent simulations of truncated xNLCME and find the small-amplitude near-band-edge gap solitons to be robust to both numerical errors and the NLS approximation.

*Department of Mathematics and Statistics, McMaster University, Hamilton, Ontario, Canada, L8S 4K1

†Department of Mathematics, University of Toronto, Toronto, Ontario, Canada, M5S 2P8

‡Department of Applied Physics and Applied Mathematics, Columbia University, New York, NY, USA, 10027

1 Introduction and Overview

Nonlinear waves in periodic structures have been a subject of great interest for many years. Early interest arose from the possibility of balancing the *band dispersion* of the periodic structure with the nonlinearity to form soliton-like structures; see, for example, [6, 10] and references cited therein. While such a heterogeneous medium possesses the same soliton-producing ingredients of dispersion and nonlinearity as found in the well known Korteweg–de Vries (KdV) and nonlinear Schrödinger (NLS) equations which govern nonlinear dispersive waves in spatially homogeneous media, the periodic variations of such an optical medium introduces additional possibilities. Indeed, changing the periodicity and material contrasts of the medium may permit tuning of the dispersive properties, *e.g.* the length scale on which a soliton can form may be altered. Thus, nonlinear and periodic structures are natural candidates for device design and applications. An example is the formation of centimeter-scale *gap solitons* in periodic optical fiber gratings. Such states have been shown to propagate at a fraction of the speed of light and have been proposed in schemes for optical storage and buffering; see, for example, [11].

In the simplest setting, nonlinear electromagnetic waves in a one-dimensional periodic structure are governed by a nonlinear Maxwell equation:

$$\partial_t^2 \left(n^2(z) E + \chi |E|^2 E \right) = \partial_z^2 E. \tag{1.1}$$

Here, $\chi > 0$ is the Kerr nonlinearity coefficient, [3]. We assume a low-contrast, periodic refractive index profile, $n(z)$, with mean n_0, given by

$$n(z) = n_0 + \epsilon N(z), \quad n_0 > 0, \quad N(z) = N(z + 2\pi), \quad 0 < \epsilon \ll 1; \tag{1.2}$$

$n(z)$ is real-valued; no energy-dissipation has been included. The fluctuating part of the refractive index, $N(z)$, can be expanded in the Fourier series

$$N(z) \equiv \sum_{p \in \mathbb{Z}} N_p e^{\mathrm{i}pz}, \quad N_{-p} = \bar{N}_p, \quad p \in \mathbb{Z}. \tag{1.3}$$

For simplicity, let us assume $N_2 \neq 0$. Then strong dispersion is excited by initial conditions of wave-packet type, *i.e.* a slowly modulated plane wave of a single frequency, chosen to be in (Bragg) resonance with the π-periodicity of the medium:

$$E(z, t = 0) = \epsilon^{\frac{1}{2}} \left[E_1^+(\epsilon z, 0) e^{\mathrm{i}z} + E_1^-(\epsilon z, 0) e^{-\mathrm{i}z} + \text{c.c.} \right], \tag{1.4}$$

where $E_1^{\pm}(Z, 0)$ are spatially localized in $Z = \epsilon z$. This resonance strongly couples backward and forward propagating waves. In the choice of initial condition (1.4), dispersive effects which are set by the medium contrast, of size $\mathcal{O}(\epsilon)$, have been balanced with nonlinear effects, by choosing the amplitude to be of size $\mathcal{O}(\epsilon^{\frac{1}{2}})$.

Suppose we make a formal multiple scale expansion based on the ansatz:

$$E(z, t) = \epsilon^{\frac{1}{2}} \left[E_1^+(Z, T) e^{\mathrm{i}(z - v_g t)} + E_1^-(Z, T) e^{-\mathrm{i}(z + v_g t)} + \text{c.c.} + \mathcal{O}(\epsilon) \right], \tag{1.5}$$
$$T = \epsilon t, \quad Z = \epsilon z, \quad v_g \equiv 1/n_0$$

Then if we only account for the principal harmonics, we shall arrive at the nonlinear coupled mode equations (NLCME) for $E_1^{\pm}(Z,T)$:

$$\partial_T E_1^+ + v_g \partial_Z E_1^+ = \mathrm{i} v_g^2 \left(N_0 E_1^+ + N_2 E_1^- \right) + \mathrm{i}\Gamma \left(|E_1^+|^2 + 2|E_1^-|^2 \right) E_1^+, \tag{1.6a}$$

$$\partial_T E_1^- - v_g \partial_Z E_1^- = \mathrm{i} v_g^2 \left(\bar{N}_2 E_1^+ + N_0 E_1^- \right) + \mathrm{i}\Gamma \left(|E_1^-|^2 + 2|E_1^+|^2 \right) E_1^-, \tag{1.6b}$$

where $\Gamma \equiv 3\chi/(2n_0^3)$. $E_1^{\pm}$ denote slowly varying forward and backward wave amplitudes; see [6] and references cited therein for details.

NLCME has been rigorously derived as a leading order model in numerous contexts. For one-dimensional propagation of electromagnetic waves in nonlinear and periodic media, it was rigorously derived from the anharmonic Maxwell-Lorenz model in [12]. Derivations from the Klein-Fock as well as Gross-Pitaevskii equations have also been obtained; see [13, 14, 16, 17]. Explicit localized stationary solutions, called *gap solitons*, for NLCME are given in [1,4] The linear stability of the gap solitons was studied in [5], and a linear, multi-dimensional, analog of NLCME was examined in [2].

However, NLCME is *not* the correct mathematical description of weakly nonlinear and weakly dispersive waves in the nonlinear and periodic Maxwell equation (1.1), (1.2). The deficiency of the NLCME system, (1.6), stems from the unperturbed ($\epsilon = 0$) equation being the *non-dispersive* one-dimensional wave equation. Due to nonlinearity, a single frequency initial condition, (1.4), excites infinitely many resonances, since $e^{\mathrm{i}m(z \pm t/n_0)}, m \in \mathbb{Z}$ all lie in the kernel of the unperturbed operator, $n_0^2 \partial_t^2 - \partial_z^2$. In contrast, other models, such as the aforementioned anharmonic Maxwell-Lorenz system and the Gross-Pitaevskii equation, remain dispersive in the $\epsilon = 0$ limit; this precludes infinitely many resonant modes.

In [19], nonlocal equations derived from nonlinear geometrical optics and an equivalent system of infinitely many coupled PDEs, which take into account the infinitely many resonances, were systematically studied. One begins with the general weakly nonlinear ansatz,

$$E(z,t) = \epsilon^{\frac{1}{2}} \left[E^+(Z,T,z - v_g t) + E^-(Z,T,z + v_g t) + \mathcal{O}(\epsilon) \right], \tag{1.7}$$

which need not be nearly monochromatic. A necessary condition for the error term in (1.7) to be of order ϵ on the time interval $0 \le t \le \mathcal{O}\left(\epsilon^{-1}\right)$ is that the forward and backward wave components, $E^{\pm}(Z,T,\phi_{\pm})$, $\phi_{\pm} = z \mp v_g t$, satisfy the system of nonlocal evolution equations:

$$\begin{aligned}(\partial_T + v_g \partial_Z + v_g^2 N_0 \partial_\phi) E^+ = {} & v_g^2 \partial_\phi \left[\frac{1}{2\pi} \int_{-\pi}^{\pi} N(\phi + \theta) E^-(Z,T,\phi + 2\theta) d\theta \right] \\ & + \frac{\Gamma}{3} \partial_\phi \left[(E^+)^3 + 3 \left(\frac{1}{2\pi} \int_{-\pi}^{\pi} |E^-(Z,T,\theta)|^2 d\theta \right) E^+ \right],\end{aligned} \tag{1.8a}$$

$$\begin{aligned}(\partial_T - v_g \partial_Z - v_g^2 N_0 \partial_\phi) E_p^- = {} & -v_g^2 \partial_\phi \left[\frac{1}{2\pi} \int_{-\pi}^{\pi} N(\phi - \theta) E^+(Z,T,\phi - 2\theta) d\theta \right] \\ & - \frac{\Gamma}{3} \partial_\phi \left[(E^-)^3 + 3 \left(\frac{1}{2\pi} \int_{-\pi}^{\pi} |E^+(Z,T,\theta)|^2 d\theta \right) E^- \right].\end{aligned} \tag{1.8b}$$

While we have omitted the $\pm$ subscripts on ∂_ϕ derivatives for the sake of brevity, the reader should note that in recovering the primitive field, as in (1.7), E^+ must be evaluated at ϕ_+ and E^- must be evaluated at ϕ_-. $E^\pm(Z,T,\phi_\pm)$ are assumed to be 2π-periodic in their $\phi_\pm$ arguments. A similar, but more general system of integro-differential equations was obtained in [19], though in that work, the authors set $N_0 = 0$ and $v_g = 1$.

If we expand $E^\pm(Z,T,\phi)$ in a Fourier series with respect to the phase variable ϕ,

$$E^\pm(Z,T,\phi) = \sum_{p\in\mathbb{Z}} E_p^\pm(Z,T) e^{\pm \mathrm{i}p\phi}, \tag{1.9}$$

the nonlocal system (1.8) may be re-expressed as a system of *infinitely* many nonlinear coupled mode (differential) equations for the Fourier mode coefficients, indexed by $p \in \mathbb{Z}$:

$$\begin{aligned}
\partial_T E_p^+ + v_g \partial_Z E_p^+ &= \mathrm{i}p v_g^2 (N_0 E_p^+ + N_{2p} E_p^-) \\
&\quad + \mathrm{i}p \frac{\Gamma}{3} \left[\sum_{q,r\in\mathbb{Z}} E_q^+ E_r^+ \bar{E}_{q+r-p}^+ + 3 \left(\sum_{q\in\mathbb{Z}} |E_q^-|^2 \right) E_p^+ \right], \qquad (1.10a) \\
\partial_T E_p^- - v_g \partial_Z E_p^- &= \mathrm{i}p v_g^2 (N_{-2p} E_p^+ + N_0 E_p^-) \\
&\quad + \mathrm{i}p \frac{\Gamma}{3} \left[\sum_{q,r\in\mathbb{Z}} E_q^- E_r^- \bar{E}_{q+r-p}^- + 3 \left(\sum_{q\in\mathbb{Z}} |E_q^+|^2 \right) E_p^- \right]. \qquad (1.10b)
\end{aligned}$$

In [19] the infinite system of PDEs (1.10) is referred to as the *extended nonlinear coupled mode equations* or xNLCME. Thus xNLCME is an extension of the classical NLCME (1.6), appropriate for *highly resonant* settings, such as the weakly periodic and nonlinear Maxwell model (1.1). Truncation of xNLCME to a single mode, $E_1^\pm(Z,T)$, yields NLCME, (1.6), which, as noted, has spatially localized gap-soliton solutions.

Numerical simulations of the primitive nonlinear and periodic Maxwell's equations, (1.1), give evidence of two phenomena. First, there appear to be long-lived spatially localized coherent structures. Second, within such spatially localized structures, a train of *carrier shocks* can form. These structures appear to be well described by xNLCME, [19].

The nonlinear Maxwell equation, (1.1), does not incorporate any effects of chromatic dispersion which, as in the anharmonic Maxwell-Lorentz model [12], *takes off resonance* the higher harmonics. However, chromatic dispersion on the length scales of many experiments is a negligible effect, [9]. Moreover, there are experimentally realizable regimes in which pulses with spectral content near the zero dispersion point are propagated [15]. In these experiments, a broad band *super continuum* is generated. The carrier shocking mentioned above is a possible source of such broad band emission.

In this paper, we explore, by analytical, asymptotic and numerical methods, the existence and properties of spatially localized structures of xNLCME. These coherent solutions have a full spectrum of active temporal frequencies and we therefore refer to them as *broad band solitons*. An earlier step in this direction was taken in [20], where the authors studied what amounts to a truncation of xNLCME to first and third harmonics. Studying the

problem numerically, they found evidence for spatially localized solutions that they called *polychromatic* solitons.

We focus on the stationary, small amplitude, near band edge, approximation of xNLCME for a particular refractive index consisting of an infinite periodic array of Dirac delta functions. In this regime, xNLCME is well-approximated by an infinite system of coupled nonlinear Schrödinger equations, the *extended nonlinear Schrödinger system*, xNLS. We embed xNLS in a one-parameter family of equations, xNLS$^\epsilon$, which continuously interpolates between a system of infinitely many decoupled NLS equations ($\epsilon = 0$) and xNLS ($\epsilon = 1$). Using bifurcation methods, based on the Lyapunov-Schmidt method and the implicit function theorem, we prove the existence of solutions for a range of $\epsilon \in (-\epsilon_0, \epsilon_0)$. By numerical continuation method, we establish the persistence of certain branches all the way to $\epsilon = 1$ for finite truncations of xNLS$^\epsilon$. Finally, we perform time-dependent simulations of xNLCME and find the small amplitude near band edge gap solitons to be robust.

Outline of the paper: In Section 2, we present a direct derivation of xNLCME in the case of a periodic medium and show the sense in which xNLCME is an infinite dimensional Hamiltonian system. In Section 3 we heuristically determine conditions on $N(z)$ for which we may expect exponentially localized gap solitons. This motivates us to focus on the case where $N(z)$ is a periodic array of delta functions.

In the small amplitude, near band edge, limit where xNLCME reduces to xNLS, we conjecture that localized stationary solutions of xNLS exist. Subject to this assumption, we prove in Theorem 1 that the gap soliton persists within xNLCME, in the asymptotic limit. Since the energy of xNLS is bounded below, it is natural to ask where a ground state of xNLS can be constructed variationally. Unfortunately, standard methods to not apply due to a loss of compactness, illustrated in Section 3.2.3. The existence of nontrivial critical points is an open problem.

We therefore seek to construct localized states via a continuation method. First, we embed xNLS in a one-parameter family of systems, xNLS$^\epsilon$, with $\epsilon = 0$ corresponding to an infinite system of decoupled NLS equations and $\epsilon = 1$ corresponding to xNLS, the system of interest. In Theorem 2, we prove the existence of gap solitons for xNLS$^\epsilon$ for an open interval of $|\epsilon| < \epsilon_0$ about $\epsilon = 0$.

We next attempt to numerically continue xNLS$^\epsilon$ solitons on the interval $[0, 1]$. In order to implement the numerical continuation, we seek approximate critical points of the xNLS$^\epsilon$ variational problem. To motivate this, in Section 4, we replace the variational characterization of xNLS$^\epsilon$ solitons by a finite dimensional minimization problem over families of Gaussian trial functions. We find critical points, with sign alternating amplitudes, of such finite dimensional approximations and give convincing numerical evidence that some can be continued to $\epsilon = 1$.

In Section 5 we compute soliton solutions of truncated xNLS using information gleaned from the trial function approximations, and show that they are robust in time-dependent simulations of truncated. Section 6 summarizes our findings and highlights open problems.

Acknowledgements: DP and GS were supported by NSERC. MIW was supported in part by US-NSF grants DMS-07-07850 and DMS-10-08855.

2 Coupled Mode Equations

In Section 2.1, we present a derivation of xNLCME from Maxwell's equations using Fourier expansions of $E^{\pm}(Z,T,\phi_{\pm})$, in the case where $E^{\pm}(Z,T,\phi_{\pm})$ are periodic in $\phi_{\pm}$. In Section 2.2, we demonstrate that xNLCME is an infinite dimensional Hamiltonian system with two conserved quantities.

2.1 Derivation of xNLCME in a Periodically Varying Medium

For simplicity and without loss of generality, we set $n_0 = 1$ so that $v_g \equiv 1$. We rewrite the nonlinear Maxwell equation (1.1) with refractive index (1.2) as

$$\partial_z^2 E - \partial_t^2 E = 2\epsilon N(z)\partial_t^2 E + \epsilon^2 N(z)^2 \partial_t^2 E + \chi \partial_t^2 |E|^2 E, \tag{2.1}$$

For $\epsilon = 0$ and $\chi = 0$, (2.1) simplifies to the one dimensional wave equation with a solution, given by the arbitrary superposition of right and left traveling waves,

$$E^{(0)}(z,t) = E^{+}(z-t) + E^{-}(z+t). \tag{2.2}$$

For ϵ small, we seek $E = E^{\epsilon}(z,t)$ in the form of a multiple scale expansion

$$E(z,t) = \epsilon^{\frac{1}{2}} \left(E^{(0)}(Z,T;z,t) + \epsilon E^{(1)}(Z,T;z,t) + \mathcal{O}(\epsilon^2) \right), \tag{2.3}$$

where $Z = \epsilon z$ and $T = \epsilon t$ are slow spatial and temporal scales. Substituting (2.3) into (2.1), we obtain at first order in ϵ:

$$\left(\partial_z^2 - \partial_t^2\right) E^{(1)} = 2\left(\partial_t \partial_T - \partial_z \partial_Z\right) E^{(0)} + 2N(z)\partial_t^2 E^{(0)} + \chi \partial_t^2 |E^{(0)}|^2 E^{(0)}. \tag{2.4}$$

The right-hand-side of (2.4) generates resonant terms along the characteristics of the wave equation, leading to secular growth of the correction $E^{(1)}$ in (z,t). The slow evolution in (Z,T) is determined to remove these secular terms.

We begin by expanding E in a Fourier series:

$$E^{\pm}(Z,T;z,t) = \sum_{p\in\mathbb{Z}} E_p^{\pm}(Z,T) e^{\pm \mathrm{i}p(z\mp t)}, \quad E^{(1)}(Z,T;z,t) = \sum_{p\in\mathbb{Z}} E_p^{(1)}(Z,T;t) e^{\mathrm{i}pz}. \tag{2.5}$$

Since $E^{\pm}$ are real-valued,

$$\bar{E}_p^{\pm}(Z,T) = E_{-p}^{\pm}(Z,T), \quad p \in \mathbb{Z}. \tag{2.6}$$

Substituting (2.5) into (2.4), the terms of the equation proportional to e^{ipz} are:

$$\begin{aligned}\left(\partial_t^2+p^2\right)E_p =& 2ip(\partial_T+\partial_Z)E_p^+e^{-ipt}-2ip(\partial_T-\partial_Z)E_{-p}^-e^{ipt}\\ &+2\sum_q q^2\left(N_{p-q}E_q^+e^{-iqt}+N_{p+q}E_q^-e^{-iqt}\right)\\ &+\chi\sum_{q,r}p^2E_q^+E_r^+\bar{E}_{q+r-p}^+e^{-ipt}+2\chi\sum_{q,r}(p-2q+2r)^2E_q^+\bar{E}_r^+E_{q-r-p}^-e^{i(p-2q+2r)t}\\ &+\chi\sum_{q,r}(p+2q+2r)^2E_q^-E_r^-\bar{E}_{-p-q-r}^+e^{-i(p+2q+2r)t}\\ &+\chi\sum_{q,r}(p-2q-2r)^2E_q^+E_r^+\bar{E}_{p-q-r}^-e^{i(p-2q-2r)t}\\ &+2\chi\sum_{q,r}(p+2q-2r)^2E_q^-\bar{E}_r^-E_{p+q-r}^+e^{-i(p+2q-2r)t}+\chi\sum_{q,r}p^2E_q^-\bar{E}_r^-E_{-p-q+r}^-e^{ipt},\end{aligned}$$

where all sums are taken over $\mathbb{Z}$. Removing the terms resonant with e^{ipt}, we obtain

$$\begin{aligned}(\partial_T+\partial_Z)E_p^+ =& ip\left(N_0E_p^++N_{2p}E_p^-\right)\\ &+ip\frac{\Gamma}{3}\left[\sum_{q,r}E_q^+E_r^+\bar{E}_{q+r-p}^++2E_0^-\sum_q E_q^+\bar{E}_{q-p}^+\right.\\ &\left.+\sum_q E_q^-E_{-q}^-\bar{E}_{-p}^++\bar{E}_0^-\sum_q E_q^+E_{p-q}^++2\sum_q|E_q^-|^2E_p^+\right].\end{aligned}\tag{2.7a}$$

Removing terms resonant with e^{-ipt}, we obtain

$$\begin{aligned}-(\partial_T-\partial_Z)E_{-p}^- =& ip\left(N_{2p}E_{-p}^++N_0E_{-p}^-\right)\\ &+ip\frac{\Gamma}{3}\left[\sum_{q,r}E_q^-E_r^-\bar{E}_{q+r+p}^-+2E_0^+\sum_q E_q\bar{E}_{p+q}^-\right.\\ &\left.+\sum_q E_q^+E_{-q}^+\bar{E}_p^-+\bar{E}_0^+\sum_q E_q\bar{E}_{-p-q}^++2\sum_q|E_q^+|^2E_{-p}^-\right]\end{aligned}\tag{2.7b}$$

where we have set $\Gamma\equiv 3\chi/2$ to be consistent with previous work, [12, 19]. Exchanging p for $-p$ in (2.7b), we have

$$\begin{aligned}(\partial_T-\partial_Z)E_p^- =& ip\left(N_{-2p}E_p^++N_0E_p^-\right)\\ &+ip\frac{\Gamma}{3}\left[\sum_{q,r}E_q^-E_r^-\bar{E}_{q+r-p}^-+2E_0^+\sum_q E_q\bar{E}_{-p+q}^-\right.\\ &\left.+\sum_q E_q^+E_{-q}^+\bar{E}_{-p}^-+\bar{E}_0^+\sum_q E_q\bar{E}_{p-q}^++2\sum_q|E_q^+|^2E_p^-\right]\end{aligned}$$

At $p = 0$, (2.7) can be satisfied by choosing arbitrary functions $E_0^{\pm} = E_0^{\pm}(Z \mp T)$. For simplicity, we set $E_0^{\pm}(Z \mp T) \equiv 0$. If we additionally invoke complex conjugate relationship (2.6), (2.7) simplify to xNLCME, (1.10), from the introduction, provided $v_g = 1$.

Finally, the nonlocal system (1.8) can be recovered by introducing the identities

$$E^{\pm}(Z,T,\phi) = \sum_{p\in\mathbb{Z}} E_p^{\pm}(Z,T)e^{\pm \mathrm{i}p\phi}, \quad E_p^{\pm}(Z,T) = \frac{1}{2\pi}\int_{-\pi}^{\pi} E^{\pm}(Z,T,\phi)e^{\mp \mathrm{i}p\phi}d\phi. \tag{2.8}$$

Constraints (2.6) imply that $E^{\pm}$ are real-valued. Note that in the context of the primitive electric field variables, $E^{\pm}(Z,T,\phi_{\pm})$ must be evaluated at different phases, $\phi_{\pm} = z \mp t$.

2.2 Hamiltonian Structure of xNLCME

Let $E_0^{\pm}$, and define $H = \int_{\mathbb{R}} \mathcal{H} dZ$, where

$$\begin{aligned}
\mathcal{H} = {} & \frac{\mathrm{i}}{2}\sum_p \frac{1}{p}\left(E_p^+\partial_Z\bar{E}_p^+ - E_p^-\partial_Z\bar{E}_p^- - \bar{E}_p^+\partial_Z E_p^+ + \bar{E}_p^-\partial_Z E_p^-\right) \\
& - N_0\sum_p(|E_p^+|^2 + |E_p^-|^2) - \sum_p N_{2p}(\bar{E}_{-p}^- E_{-p}^+ + E_p^-\bar{E}_p^+) \\
& - \frac{\Gamma}{6}\left(\sum_p \bar{E}_p^+\bar{E}_{-p}^+\right)\left(\sum_p E_p^- E_{-p}^-\right) - \frac{\Gamma}{6}\left(\sum_p \bar{E}_p^-\bar{E}_{-p}^-\right)\left(\sum_p E_p^+ E_{-p}^+\right) \\
& - \frac{\Gamma}{6}\sum_{p,q,r}\left(\bar{E}_p^+ E_q^+ E_r^+ \bar{E}_{q+r-p}^+ + \bar{E}_p^- E_q^- E_r^- \bar{E}_{q+r-p}^-\right) - \frac{2\Gamma}{3}\left(\sum_p |E_p^+|^2\right)\left(\sum_p |E_p^-|^2\right),
\end{aligned} \tag{2.9}$$

with all sums are over $\mathbb{Z}\setminus\{0\}$. Then, xNLCME has the structure of an infinite dimensional Hamiltonian system:

$$\partial_T E_p^+ = -\mathrm{i}p\frac{\delta H}{\delta \bar{E}_p^+}, \quad \partial_T E_p^- = -\mathrm{i}p\frac{\delta H}{\delta \bar{E}_p^-}, \quad p \in \mathbb{Z}\setminus\{0\}. \tag{2.10}$$

Formally, the Hamiltonian (2.9) is conserved under the flow of xNLCME. Besides the Hamiltonian, the total power $N = \int_{\mathbb{R}} \mathcal{N} dZ$ is invariant, where the density is

$$\mathcal{N} = \sum_{p\in\mathbb{Z}}\left(|E_p^+|^2 + |E_p^-|^2\right). \tag{2.11}$$

This follows by direct computation.

Since $N_{2p} = \bar{N}_{-2p}$, $p \in \mathbb{Z}$, the symmetry of equations (1.10) implies that if the constraint $\bar{E}_p^{\pm} = E_{-p}^{\pm}$, associated with real initial conditions for $E^{\pm}$, is satisfied at $T = 0$, then it is satisfied for all T. Additionally, if $E_p^{\pm}$ are zero initially for even p, they remain zero for all time. This allows us to restrict (1.10) to the odd harmonics, $p \in \mathbb{Z}_{\mathrm{odd}}$, and set

$$E_p^{\pm} = 0, \quad p \in \mathbb{Z}_{\mathrm{even}}. \tag{2.12}$$

Under these constraints, the conserved integral (2.9) reduces to the Hamiltonian:

$$\begin{aligned}\mathcal{H} = &\frac{\mathrm{i}}{2}\sum_{p\in\mathbb{Z}_{\rm odd}}\frac{1}{p}\left(E_p^+\partial_Z\bar{E}_p^+ - E_p^-\partial_Z\bar{E}_p^- - \bar{E}_p^+\partial_Z E_p^+ + \bar{E}_p^-\partial_Z E_p^-\right)\\ &- N_0\sum_{p\in\mathbb{Z}_{\rm odd}}(|E_p^+|^2+|E_p^-|^2) - 2\sum_{p\in\mathbb{Z}_{\rm odd}}N_{2p}E_p^-\bar{E}_p^+\\ &- \Gamma\left(\sum_{p\in\mathbb{Z}_{\rm odd}}|E_p^+|^2\right)\left(\sum_{p\in\mathbb{Z}_{\rm odd}}|E_p^-|^2\right)\\ &- \frac{\Gamma}{6}\sum_{p,q,r\in\mathbb{Z}_{\rm odd}}\left(\bar{E}_p^+E_q^+E_r^+\bar{E}_{q+r-p}^+ + \bar{E}_p^-E_q^-E_r^-\bar{E}_{q+r-p}^-\right).\end{aligned} \tag{2.13}$$

As in the case of standard NLCME, (2.13) is unbounded from above and below subject to the constraint of fixed $\mathcal{N}$. Thus, critical points are expected to be of *infinite index*. This suggests that variational methods will be of limited applicability for studying the stability of localized stationary states of xNLCME.

3 Gap Solitons

We now begin to explore the existence of localized stationary states of xNLCME (1.10), called *gap solitons*. Setting $v_g = 1$ for convenience, we seek solutions of the form

$$E_p^+(Z,T) = e^{\mathrm{i}p(N_0-\Omega)T}A_p(Z), \quad E_p^-(Z,T) = e^{\mathrm{i}p(N_0-\Omega)T}B_p(Z), \quad p\in\mathbb{Z}, \tag{3.1}$$

where Ω is a real frequency parameter and $\{A_p(Z), B_p(Z)\}_{p\in\mathbb{Z}}$ are complex-valued amplitudes. Using constraints (2.6) and (2.12), we assume

$$A_p = \bar{A}_{-p}, \quad B_p = \bar{B}_{-p}, \quad p\in\mathbb{Z}_{\rm odd}, \quad A_p = B_p = 0, \quad p\in\mathbb{Z}_{\rm even}. \tag{3.2}$$

The infinite family of amplitudes $\{A_p, B_p\}_{p\in\mathbb{Z}_{\rm odd}}$ satisfies the extended system of stationary equations

$$\mathrm{i}A_p'(Z) + p\Omega A_p + pN_{2p}B_p + p\frac{\Gamma}{3}\left(3A_p\sum_{q\in\mathbb{Z}_{\rm odd}}|B_q|^2 + \sum_{q,r\in\mathbb{Z}_{\rm odd}}A_qA_rA_{p-q-r}\right) = 0, \tag{3.3a}$$

$$-\mathrm{i}B_p'(Z) + p\Omega B_p + p\bar{N}_{2p}A_p + p\frac{\Gamma}{3}\left(3B_p\sum_{q\in\mathbb{Z}_{\rm odd}}|A_q|^2 + \sum_{q,r\in\mathbb{Z}_{\rm odd}}B_qB_rB_{p-q-r}\right) = 0, \tag{3.3b}$$

with constraints (3.2). Linearizing about the zero solution yields decoupled systems of differential equations with solutions

$$\begin{bmatrix} A_p \\ B_p \end{bmatrix} \sim e^{\pm Z\sqrt{|pN_p|^2-(p\Omega)^2}}, \quad p\in\mathbb{Z}_{\rm odd}. \tag{3.4}$$

A sufficient condition for spatial localization near the zero solution is only possible if $|\Omega| < \Omega_0 \equiv \min_{p\in\mathbb{Z}_{\rm odd}}|N_{2p}|$, implying three possibilities:

Case 1, $\Omega_0 > 0$**:** An example would be $N_{2p} = 1$, $p \in \mathbb{Z}$, in which case the refractive index, $N(z)$, is a periodic sequence of Dirac delta-functions.

Case 2, $\Omega_0 = 0$ **and** $\min_{p\in\mathbb{Z}_{\text{odd}}} |pN_{2p}| > 0$**:** An example would be $N_{2p} = p^{-1}$, $p \in \mathbb{Z}_{\text{odd}}$, for which $N(z)$ would correspond to a periodic sequence of step functions.

Case 3, $\Omega_0 = 0$ **and** $\min_{p\in\mathbb{Z}_{\text{odd}}} |p^2 N_{2p}| < \infty$**:** In this case, $N(z)$ is continuous.

If $N_{2p} = 1$, $p \in \mathbb{Z}_{\text{odd}}$, the band gap of each mode is opened, and the widths of the band gaps grow as $|p| \to \infty$. However, because of the coupling between the Fourier modes with amplitudes $\{A_p, B_p\}_{p\in\mathbb{Z}_{\text{odd}}}$, the stationary localized mode (gap soliton) may only reside in the gap of a fixed width, $|\Omega| < \Omega_0 \equiv 1$.

If $N_{2p} = \mathcal{O}(|p|^{-1})$, the band gap of each mode is again opened, but the widths are nearly constant as $|p| \to \infty$. However, the band gap for the coupled gap soliton shrinks now to zero and the parameter Ω must be set to 0.

If $N_{2p} = \mathcal{O}(|p|^{-2})$, the widths of the band gaps shrink with the larger values of p, and the exponential decay (3.4) ceases as $|p| \to \infty$, even if $\Omega = 0$. We do not anticipate the existence of gap solitons in this case.

We now restrict our attention to Case 1: $\Omega_0 > 0$ and set $N_{2p} = 1$ for all $p \in \mathbb{Z}_{\text{odd}}$. System (3.3) can now be rewritten as an equivalent integro-differential equation:

$$(-\partial_Z + \Omega\partial_\phi)A + \partial_\phi B + \frac{\Gamma}{3}\partial_\phi \left[A^3 + 3\left(\frac{1}{2\pi}\int_{-\pi}^{\pi} |B(Z,s)|^2 ds\right) A\right] = 0, \tag{3.5a}$$

$$(\partial_Z + \Omega\partial_\phi)B + \partial_\phi A + \frac{\Gamma}{3}\partial_\phi \left[B^3 + 3\left(\frac{1}{2\pi}\int_{-\pi}^{\pi} |A(Z,s)|^2 ds\right) B\right] = 0, \tag{3.5b}$$

where we have introduced the two Fourier series,

$$A(Z,\phi) = \sum_{p\in\mathbb{Z}_{\text{odd}}} A_p(Z)e^{\mathrm{i}p\phi}, \quad B(Z,\phi) = \sum_{p\in\mathbb{Z}_{\text{odd}}} B_p(Z)e^{\mathrm{i}p\phi}. \tag{3.6}$$

We note that if one wishes to compute the primitive electric field induced by these envelopes, care must be taken in where the phase variable, ϕ, is evaluated. Indeed, the electric field associated with $\{A_p, B_p\}_{p\in\mathbb{Z}_{\text{odd}}}$ is given by

$$\begin{aligned} E(z,t) &= \epsilon^{\frac{1}{2}}\left[\sum_{p\in\mathbb{Z}_{\text{odd}}} e^{\mathrm{i}p(N_0-\Omega)\epsilon t}e^{\mathrm{i}p(z-t)}A_p(\epsilon z) + \sum_{p\in\mathbb{Z}_{\text{odd}}} e^{\mathrm{i}p(N_0-\Omega)\epsilon t}e^{-\mathrm{i}p(z+t)}B_p(\epsilon z) + \mathcal{O}(\epsilon)\right] \\ &= \epsilon^{\frac{1}{2}}\left[A(\epsilon z, (N_0-\Omega)\epsilon t + z - t) + B(\epsilon z, (N_0-\Omega)\epsilon t - (z+t)) + \mathcal{O}(\epsilon)\right], \end{aligned} \tag{3.7}$$

in agreement with the ansatz (1.7).

3.1 NLCME Gap Solitons

As noted, the truncation of xNLCME to $E_1^{\pm}$ yields the classical NLCME. We now review the details of the NLCME gap soliton.

The spatial profiles of NLCME's gap soliton are given by solutions of the stationary equations:

$$\mathrm{i}A_1'(Z) + \Omega A_1 + B_1 + \Gamma(|A_1|^2 + 2|B_1|^2)A_1 = 0, \tag{3.8a}$$
$$-\mathrm{i}B_1'(Z) + \Omega B_1 + A_1 + \Gamma(2|A_1|^2 + |B_1|^2)B_1 = 0. \tag{3.8b}$$

For $\Omega \in (-1, 1)$, these equations admit the exact solutions:

$$A_1(Z) = \sqrt{\frac{2}{3\Gamma}} \frac{\mu}{\alpha \cosh(\mu Z) - \mathrm{i}\beta \sinh(\mu Z)}, \tag{3.9a}$$
$$B_1(Z) = \sqrt{\frac{2}{3\Gamma}} \frac{-\mu}{\alpha \cosh(\mu Z) + \mathrm{i}\beta \sinh(\mu Z)}, \tag{3.9b}$$

where

$$\alpha = \sqrt{1+\Omega}, \quad \beta = \sqrt{1-\Omega}, \quad \mu = \sqrt{1-\Omega^2} \equiv \alpha\beta.$$

The localized solution (3.9) satisfies the symmetry property

$$A_1(Z) = \bar{A}_1(-Z), \quad B_1(Z) = \bar{B}_1(-Z), \quad Z \in \mathbb{R}.$$

We shall call the solution of (3.9) a *monochromatic gap soliton*, since the associated approximate solution of the nonlinear Maxwell model consists of a slowing varying and localized envelope with a single fast (carrier) frequency of oscillation. This is in contrast to the broad band, or polychromatic, solitons which possess slowly varying envelopes on multiple distinct carrier frequencies. It seems unlikely that there is an explicit solution of the system (3.3) of infinitely many coupled mode equations.

3.2 Persistence of Solitons in a Band Edge Approximation

We now explore a small amplitude, spectral band edge, approximation of xNLCME, which will lead to an infinite system of coupled NLS type equations, xNLS.

3.2.1 The Band Edge Approximation

The gap in the continuous spectrum exists for $\Omega \in (-1, 1)$. In the truncated coupled mode equations (3.8), the exact solution (3.9) shows that the amplitude $\|A_1\|_{L^\infty}$ of the gap soliton becomes small as $\Omega \to 1$. Using the parameterization $\Omega = \sqrt{1-\mu^2}$ and the asymptotic expansion

$$A_1 = \mu U_1(\zeta) + \mathcal{O}(\mu^2), \quad B_1 = -\mu U_1(\zeta) + \mathcal{O}(\mu^2),$$

where $\zeta = \mu Z$ is slow variable and μ is a small parameter, we can formally reduce the system of differential equations (3.8) to the scalar second-order equation for $U_1(\zeta)$:

$$U_1''(\zeta) - U_1(\zeta) + 6\Gamma U_1^3(\zeta) = 0. \tag{3.10}$$

This equation admits the localized solution

$$U_\star(\zeta) = \frac{1}{\sqrt{3\Gamma}}\operatorname{sech}(\zeta), \tag{3.11}$$

which corresponds to the asymptotic approximation of the gap soliton (3.9) as $\Omega \to 1$.

Generalizing this approach to the system of infinitely many coupled mode equations, (3.3), we substitute $\Omega = \sqrt{1-\mu^2}$ and

$$A_p = \mu \tilde{A}_p(\zeta), \quad B_p = -\mu \tilde{B}_p(\zeta), \quad p \in \mathbb{Z}_{\text{odd}}, \tag{3.12}$$

with $\zeta = \mu Z$ into the coupled mode system (3.3) to obtain

$$\mathrm{i}\mu \tilde{A}_p' + p\sqrt{1-\mu^2}\tilde{A}_p - p\tilde{B}_p + \tfrac{p}{3}\Gamma\mu^2\tilde{F}_p = 0 \tag{3.13a}$$

$$\mathrm{i}\mu \tilde{B}_p' - p\sqrt{1-\mu^2}\tilde{B}_p + p\tilde{A}_p - \tfrac{p}{3}\Gamma\mu^2\tilde{G}_p = 0, \tag{3.13b}$$

where

$$\tilde{F}_p = 3\tilde{A}_p \sum_{q\in\mathbb{Z}_{\text{odd}}} |\tilde{B}_q|^2 + \sum_{q,r\in\mathbb{Z}_{\text{odd}}} \tilde{A}_q\tilde{A}_r\tilde{A}_{p-q-r}, \tag{3.14a}$$

$$\tilde{G}_p = 3\tilde{B}_p \sum_{q\in\mathbb{Z}_{\text{odd}}} |\tilde{A}_q|^2 + \sum_{q,r\in\mathbb{Z}_{\text{odd}}} \tilde{B}_q\tilde{B}_r\tilde{B}_{p-q-r}, \tag{3.14b}$$

Introducing the variables

$$\tilde{U}_p = \frac{\tilde{A}_p + \tilde{B}_p}{2}, \quad \tilde{V}_p = \frac{\tilde{A}_p - \tilde{B}_p}{2},$$

the system (3.13) can be written as

$$2p\tilde{V}_p + \mathrm{i}\mu\tilde{U}_p' + \left(\sqrt{1-\mu^2} - 1\right) p\tilde{V}_p + \frac{1}{6}\Gamma\mu^2 p(\tilde{F}_p - \tilde{G}_p) = 0, \tag{3.15a}$$

$$\mathrm{i}\tilde{V}_p' + \frac{\sqrt{1-\mu^2}-1}{\mu} p\tilde{U}_p + \frac{1}{6}\Gamma\mu p(\tilde{F}_p + \tilde{G}_p) = 0, \tag{3.15b}$$

where $\tilde{F}_p$, $\tilde{G}_p$ are rewritten after the substitution of the new variables.

Now, if we formally expand in powers of μ,

$$\tilde{U}_p = U_p + \mathcal{O}(\mu^1), \quad \tilde{V}_p = -\frac{\mathrm{i}\mu}{2p}U_p' + \mathcal{O}(\mu^2), \tag{3.16}$$

we find obtain, at leading order, an infinite system of coupled NLS type equations, that we deem xNLS:

$$U_p''(\zeta) - p^2 U_p + \frac{2p^2}{3}\Gamma\left(3U_p \sum_{q\in\mathbb{Z}_{\rm odd}} |U_q|^2 + \sum_{q\in\mathbb{Z}_{\rm odd}}\sum_{r\in\mathbb{Z}_{\rm odd}} U_q U_r U_{p-q-r}\right) = 0, \quad p\in\mathbb{Z}. \tag{3.17}$$

This can be rewritten as the integro-differential equation

$$(\partial_\zeta^2 + \partial_\phi^2)U = \frac{2}{3}\Gamma\partial_\phi^2\left[U^3 + 3\left(\frac{1}{2\pi}\int_{-\pi}^{\pi}|U(\zeta,\theta)|^2 d\theta\right)U\right], \tag{3.18}$$

after introducing the Fourier relations

$$U(\zeta,\phi) = \sum_{p\in\mathbb{Z}_{\rm odd}} U_p(\zeta)e^{ip\phi}, \quad U_p(\zeta) = \frac{1}{2\pi}\int_{-\pi}^{\pi} U(\zeta,\phi)e^{-ip\phi}d\phi.$$

We will now justify the reduction to xNLS, (3.17).

3.2.2 Preliminaries

We first introduce appropriate function spaces in which we study the problem. Let $\mathbb{T}$ denote the interval $[0,2\pi]$, with endpoints identified so that functions on $\mathbb{T}$ are understood to be 2π-periodic. We shall consider functions defined on $\mathbb{R}\times\mathbb{T}$, admitting the Fourier representation

$$U(\zeta,\phi) = \sum U_p(\zeta)e^{{\rm i}p\phi}.$$

For any s, the function space X^s is defined by

$$X^s \equiv \left\{ U(\zeta,\phi)\in H^s(\mathbb{R}\times\mathbb{T}): \quad \begin{array}{l} \bar{U}(\zeta,\phi) = U(\zeta,\phi), \\ \displaystyle\int_{-\pi}^{\pi} U(\zeta,\phi)\cos(2p\phi)d\phi = 0, \ \ \forall\zeta\in\mathbb{R}, p\in\mathbb{N} \end{array}\right\} \tag{3.19}$$

and equipped with the norm

$$\|U\|_{X^s} \equiv \left(\sum_{p\in\mathbb{Z}_{\rm odd}}\int_{\mathbb{R}}(p^2+\xi^2)^s|U_p(\xi)|^2 d\xi\right)^{1/2}. \tag{3.20}$$

We shall frequently go back and forth between the U and $\{U_p\}_{p\in\mathbb{Z}_{\rm odd}}$ representations of functions in X^s.

The Sobolev space $H^s(\mathbb{R}\times\mathbb{T})$ is a Banach algebra with respect to the pointwise multiplication for any $s>1$. Moreover, from the continuous embeddings $H^s(\mathbb{R}\times\mathbb{T})\hookrightarrow L^\infty(\mathbb{R}\times\mathbb{T})$ for $s>1$ and $l^2(\mathbb{Z})\hookrightarrow l^\infty(\mathbb{Z})$, we infer that if $U\in X^s$ for $s>1$, then

$$\lim_{|\zeta|\to\infty} U(\zeta,\phi) = 0, \quad \forall\phi\in\mathbb{T}. \tag{3.21}$$

Let $B_\delta(X^s)$ denote a ball of radius δ in Banach space X^s centered at the origin. The Hamiltonian H with the density (2.13) consists of the terms controlled by the H^1 norms of $E^\pm$. To see this, recall the continuous embedding $H^1(\mathbb{R}\times\mathbb{T}) \hookrightarrow L^4(\mathbb{R}\times\mathbb{T})$. It follows that for any $E^\pm \in B_\delta(X^s)$ with $s \geq 1$, there is a constant $C_{\delta,s} > 0$ such that

$$H \leq \; C_{\delta,s}\left(\|E^+\|_{X^s} + \|E^-\|_{X^s}\right).$$

Furthermore, the map $(E^+, E^-) \mapsto H$ is continuous in X^s. Although we will mainly study the problem in X^s with $s > 1$, we note that the energy is well defined in X^1.

3.2.3 Proof of Result

We now rigorously justify the small amplitude approximation of (3.3) by (3.17).

Theorem 1. *Fix $s > 1$ and assume the existence of localized solution $U \in X^s$ to (3.18) satisfying the reversibility symmetry,*

$$U_p(\zeta) = \bar{U}_p(-\zeta), \quad p \in \mathbb{Z}_{\text{odd}}, \quad \zeta \in \mathbb{R}. \tag{3.22}$$

Also assume that the linearized operator of system (3.18) at U is invertible in the subspace of X^s associated with the constraint (3.22).

There exists $\mu_0 > 0$ such that for any $\mu \in (-\mu_0, \mu_0)$, the system of stationary coupled mode equations (3.3) with $\Omega = \sqrt{1-\mu^2}$ admits a unique localized solution $A, B \in X^s$ satisfying the symmetries,

$$A_p(Z) = \bar{A}_p(-Z), \quad B_p(z) = \bar{B}_p(-Z), \quad p \in \mathbb{Z}_{\text{odd}}, \quad Z \in \mathbb{R}, \tag{3.23}$$

and the bound,

$$\|A - \mu U(\mu\cdot,\cdot)\|_{X^s} + \|B + \mu U(\mu\cdot,\cdot)\|_{X^s} \leq C\mu^2. \tag{3.24}$$

Proof. First, we note that the vectors fields $\tilde{F}(A,B)$ and $\tilde{G}(A,B)$, defined by their components in (3.14), are analytic (cubic) maps from $X^s \times X^s$ to X^s for any $s > 1$. Eliminating $\tilde{U}_p$ from system (3.15), we obtain

$$p^2\tilde{V}_p - \tilde{V}_p'' = \frac{1}{6}\Gamma\left[p^2(\sqrt{1-\mu^2}-1)(\tilde{F}_p - \tilde{G}_p) - i\mu p(\tilde{F}_p' + \tilde{G}_p')\right]. \tag{3.25}$$

The right-hand side of system (3.25) defines an analytic (cubic) map from X^s to X^{s-2} for any $s > 1$, where the X^{s-2} norm is of order $\mathcal{O}(\mu)$ as $\mu \to \infty$. The left-hand side operator of system (3.25) has a bounded inverse from X^{s-2} to X^s, thanks to the zero mean constraint in X^s. By the Implicit Function Theorem, we infer that for any $\delta > 0$ and any $s > 1$, there is $\mu_0 > 0$ such that for all $\mu \in (-\mu_0, \mu_0)$ and for all $\tilde{U}$ in a ball $B_\delta(X^s)$, there is a smooth map $X^s \ni \tilde{U} \mapsto \tilde{V}[\tilde{U}] \in X^s$ which solves system (3.25) and satisfies the bound,

$$\exists C > 0: \quad \|\tilde{V}\|_{X^s} \leq C\mu, \quad \mu \in (-\mu_0, \mu_0), \;\; \tilde{U} \in B_\delta(X^s). \tag{3.26}$$

On the other hand, eliminating $\tilde{V}$ from system (3.15), we obtain

$$\tilde{U}_p'' - p^2\tilde{U}_p + \frac{1}{6}\Gamma\left[p^2(\sqrt{1-\mu^2}+1)(\tilde{F}_p+\tilde{G}_p) - i\mu p(\tilde{F}_p' - \tilde{G}_p'\right] = 0. \tag{3.27}$$

Thanks to the bound (3.26), the cubic terms of the system (3.27) are different from those of the system (3.17) by the error of the order of $\mathcal{O}(\mu^2)$ in X^{s-2}. Under the assumptions of the existence of the solution $U \in X^s$ of the truncated coupled NLS equations (3.18) and the invertibility of the linearized operator in the subspace of X^s associated with the constraint (3.22), the linearized operator has a bounded inverse from X^{s-2} to X^s for any small $\mu \in \mathbb{R}$. By the contraction mapping arguments, there is a solution $\tilde{U}$ near U in X^s such that

$$\exists C > 0: \quad \|\tilde{U} - U\|_{X^s} \leq C\mu^2.$$

This gives the statement of the theorem, after the original variables A, B, and Z are restored from the transformations above. □

3.3 Hamiltonian & Power of xNLS

The extended system of coupled nonlinear Schrödinger equations (xNLS) (3.17) inherits the Hamiltonian structure of the coupled mode equations (3.3). The energy functional for (3.17) is given by

$$H_{\text{xNLS}} = \int_{\mathbb{R}} \left[\sum_{p\in\mathbb{Z}_{\text{odd}}} \left(\frac{1}{p^2}|U_p'|^2 + |U_p|^2 \right) - \Gamma \left(\sum_{p\in\mathbb{Z}_{\text{odd}}} |U_p|^2 \right)^2 - \frac{\Gamma}{3} \sum_{p,q,r\in\mathbb{Z}_{\text{odd}}} \bar{U}_p U_q U_r \bar{U}_{q+r-p} \right] d\zeta. \tag{3.28}$$

We also define the power,

$$N_{\text{xNLS}} = \int_{\mathbb{R}} \left[\sum_{p\in\mathbb{Z}} |U_p|^2 \right] d\zeta. \tag{3.29}$$

Energy functionals are often used in proving the existence of localized solutions to constrained variational problems, *e.g.*

$$\text{minimize } H_{\text{xNLS}} \text{ subject to fixed } N_{\text{xNLS}}. \tag{3.30}$$

Unfortunately, this strategy fails for our problem, as demonstrated by the following counterexample. Let

$$U_p(\zeta) = \lambda_n^{1/2} W(\lambda_n \zeta)\left(\delta_{p,n} + \delta_{p,-n}\right), \quad p \in \mathbb{Z}_{\text{odd}}, \tag{3.31}$$

where $W \in H^1(\mathbb{R})$ is a fixed function, $\lambda_n > 0$ is an arbitrary parameter, and $n \geq 1$ is an arbitrary odd integer. Then, N_{xNLS} is independent on the parameters λ_n and n. On the other hand,

$$H_{\text{xNLS}} = \frac{2\lambda_n^2}{n^2}\|W'\|_{L^2}^2 - 6\lambda_n \|B\|_{L^4}^4.$$

If we set $\lambda_n = n$ and let $n \to \infty$, we obtain no lower bound on H_{xNLS}. Thus, localized solutions of xNLS, (3.17), if they exist in some X^s, cannot be global minimizers; they will either be local extrema or saddle points.

3.4 Persistence of Monochromatic Solitons to Coupling in xNLS

We study the question of persistence of NLS solitons within xNLS by embedding xNLS in a one-parameter family of models, xNLS$^\epsilon$, for which xNLS^0 is an infinite system of decoupled NLS equations and xNLS^1=xNLS. Our formulation is:

$$U_p''(\zeta) - p^2 U_p + 6p^2\Gamma U_p^3 + \frac{2p^2}{3}\epsilon\Gamma\left(3U_p\sum_{q\in\mathbb{Z}_{\text{odd}}}|U_q|^2 + \sum_{q,r\in\mathbb{Z}_{\text{odd}}} U_q U_r U_{p-q-r}\right) = 0, \quad p\in\mathbb{Z}_{\text{odd}}, \tag{3.32}$$

where the sums exclude the cubic self interaction terms, U_p^3. Within each mode of the decoupled system at $\epsilon = 0$, we have a solution

$$U_p(\zeta) = \pm U_\star(p\zeta), \quad p\in\mathbb{Z}_{\text{odd}}, \tag{3.33}$$

where $U_\star(\zeta)$ is the NLS soliton (3.11).

We now prove the persistence of (3.33) within xNLS$^\epsilon$, (3.32), for all ϵ sufficiently small. Without loss of generality, we can take $p = 1$. Furthermore, we make the reduction

$$U_p(\zeta) = \bar{U}_p(\zeta) = U_{-p}(\zeta), \quad , p\in\mathbb{Z}_{\text{odd}}.$$

In other words, we now assume that the envelopes in each harmonic are real-valued.

Theorem 2. *Fix $s > 1$. There exists $\epsilon_0 > 0$ and $C > 0$ such that for any $\epsilon\in(-\epsilon_0,\epsilon_0)$, xNLS, (3.32) admits a unique localized solution $U\in X^s$ satisfying the even symmetry:*

$$U_p(\zeta) = U_p(-\zeta) \tag{3.34}$$

Moreover, $U(\zeta,\phi)$ is a small deformation of the unperturbed $\epsilon = 0$ soliton solution:

$$\mathcal{U}_\star(\zeta,\phi) = 2U_\star(\zeta)\cos(\phi),$$

in the sense that

$$\|U - \mathcal{U}\|_{X^s} \le C\epsilon \tag{3.35}$$

Proof. The proof relies on a Lyapunov-Schmidt reduction where we shall first express the higher harmonics as functions of $U_1 = U_{-1}$, and then apply the implicit function theorem to an equation written entirely in terms of U_1.

From (3.32), define F in terms of the components

$$F_p = 3U_p\sum_{q\in\mathbb{Z}_{\text{odd}}}|U_q|^2 + \sum_{q,r\in\mathbb{Z}_{\text{odd}}} U_q U_r U_{p-q-r},$$

where each F_p excludes the purely self-interacting terms. For $|p| > 1$, we can clearly write

$$U_p = -(\partial_\zeta^2 - p^2)^{-1}p^2\left(6\Gamma U_p^3\right) - \epsilon(\partial_\zeta^2 - p^2)^{-1}p^2\frac{2}{3}\Gamma F_p. \tag{3.36}$$

The terms on the left are in X^s since $s > 1$ and $(\partial_\zeta^2 - p^2)^{-1}p^2$ is a bounded operator. Therefore, for sufficiently small $\epsilon_0 > 0$ and finite δ_0, the contraction mapping theorem yields a unique map,

$$\Phi : (U_1, \epsilon) \mapsto \{U_p\}_{|p|>1}$$

in a ball $U_1 \in B_\delta(H^s)$ with $\delta < \delta_0$ and $|\epsilon| < \epsilon_0$. For a given $U_1 = U_{-1}$, we have expressed the other modes in terms of this fixed profile. Form (3.36), we can see that there exists a constant $C > 0$ such that for all $|\epsilon| < \epsilon_0$,

$$\|\Phi(U_1, \epsilon)\|_{X^s} \leq C\epsilon \|U_1\|_{H^s}^3$$

We now eliminate $\{U\}_{|p|>1}$ from the $p = \pm 1$ equations of (3.32) using the mapping Φ. Since $U_1 = U_{-1}$, we only consider the $p = 1$ equation:

$$U_1'' - U_1 + 6\Gamma U_1^3 = -\frac{2}{3}\epsilon\Gamma F_1[\Phi(U_1, \epsilon)]. \tag{3.37}$$

For any $U_1 \in B_\delta(H^s)$ with finite $\delta > 0$ and small $|\epsilon| < \epsilon_0$, there is a $C > 0$ such that

$$\|F_1[\Phi(U_1, \epsilon)]\|_{H^s} \leq C\epsilon \|U_1\|_{H^s}^5.$$

To solve (3.37), we hope to apply the implicit function theorem. Thus, we must linearize (3.37) near $U_\star$ at $\epsilon = 0$, and show that it is invertible. The kernel of the linearized operator,

$$\partial_\zeta^2 - 1 + 18\Gamma U_\star^2$$

is just $\partial_\zeta U_\star$. Obviously, this does not satisfy the symmetry constraint, (3.34). Subject to this condition, the operator is an isomorphism from $H^s_{\text{even}} \to H^{s-2}_{\text{even}}$, the subspace of H^s of even functions. Hence, the implicit function theorem yields a neighborhood of $U_\star$ in H^s in which we can obtain U_1 with $|\epsilon| < \epsilon_1 \leq \epsilon_0$.

Moreover, we see from (3.37) that there exists $C > 0$ such that for all $|\epsilon| < \epsilon_1$,

$$\|U_1 - U_\star\|_{H^s} \leq C\epsilon^2$$

Combining this estimate with (3.36), yields (3.35).

□

This result has several obvious extensions. We can consider the local continuation about a soliton localized in any other mode $p_0 \in \mathbb{Z}_{\text{odd}}$,

$$U_{p_0}(\zeta) = \pm U_\star(p\zeta). \tag{3.38}$$

We could also continue a solution about any finite collection of such solitons. However, if we begin with solitons in every odd harmonic, they will not have finite L^2, as

$$\int \sum_{p\in\mathbb{Z}_{\text{odd}}} |U_p|^2 d\zeta = \|U_\star\|_{L^2}^2 \sum_{p\in\mathbb{Z}_{\text{odd}}} \frac{1}{|p|}$$

which diverges. The continuation of such infinite energy solutions is an open problem.

4 Variational Approximations

As noted at the end of Section 3.2.3, although the functional is bounded from below, the natural variational formulation for localized solutions of xNLS exhibits a loss of compactness. In this section we explore the use of this functional to obtain Rayleigh-Ritz or Galerkin-type approximations to such states. The parameters in these approximations can be uniquely determined from the conditions that the ansatz gives a stationary point of $H_{\rm xNLS}$. Indeed, variations of $H_{\rm xNLS}$ produce the Euler–Lagrange equations, which are equivalent to the differential equations (3.17).

4.1 Gaussian Approximations

Let us consider the Gaussian variational ansatz

$$U_p(\zeta) = a_p e^{-b_p \zeta^2}, \quad p \in \mathbb{Z}_{\rm odd}, \tag{4.1}$$

where $a_p \in \mathbb{R}$ and $b_p \in \mathbb{R}_+$ are parameters of the variational approximation. The Gaussian ansatz is useful because all integrals in $H_{\rm xNLS}$ can be computed in the analytical form. Direct substitution and integration show that $\sqrt{\frac{2}{\pi}} H_{\rm xNLS}$ becomes

$$H_{\rm Gauss} = \sum_{p \in \mathbb{Z}_{\rm odd}} \frac{\sqrt{b_p} a_p^2}{p^2} + \frac{a_p^2}{\sqrt{b_p}} - \Gamma \sum_{p,q \in \mathbb{Z}_{\rm odd}} \frac{a_p^2 a_q^2}{\sqrt{b_p + b_q}} - \frac{1}{3}\Gamma \sum_{p,q,r \in \mathbb{Z}_{\rm odd}} \frac{\sqrt{2} a_p a_q a_r a_{p-q-r}}{\sqrt{b_p + b_q + b_r + b_{p-q-r}}}. \tag{4.2}$$

If the artificial small parameter ϵ is introduced to decouple the different modes, as in system (3.32), then (4.2) is rewritten in the form,

$$\begin{aligned} H_{\rm Gauss}(\epsilon) \equiv & \sum_{p \in \mathbb{Z}_{\rm odd}} \frac{\sqrt{b_p} a_p^2}{p^2} + \frac{a_p^2}{\sqrt{b_p}} - \Gamma \frac{3 a_p^4}{\sqrt{2}\sqrt{b_p}} \\ & - \epsilon \Gamma \left(\sum_{p,q \in \mathbb{Z}_{\rm odd}} \frac{a_p^2 a_q^2}{\sqrt{b_p + b_q}} + \frac{1}{3} \sum_{p,q,r \in \mathbb{Z}_{\rm odd}} \frac{\sqrt{2} a_p a_q a_r a_{p-q-r}}{\sqrt{b_p + b_q + b_r + b_{p-q-r}}} \right). \end{aligned} \tag{4.3}$$

The above sums with ϵ as a prefactor exclude the purely self interacting $a_p^4/\sqrt{b_p}$ terms.

If $\epsilon = 0$, there exists an uncoupled solution of the Euler–Lagrange equations produced from variations of $H_{\rm Gauss}(0)$,

$$a_p = \pm \frac{2^{3/4}}{3\Gamma^{1/2}}, \quad b_p = \frac{p^2}{3}, \quad p \in \mathbb{Z}_{\rm odd}. \tag{4.4}$$

The exact solution (4.4) will be used as a seed point in the numerical continuation algorithm.

Table 1: Computed values for a truncated Rayleigh-Ritz approximation for $\epsilon = 1$.

No. of Modes	a_1	b_1	a_3	b_3	a_5	b_5
1	0.56060	0.33333	-	-	-	-
2	0.56321	0.33148	-0.13918	3.9413	-	-
3	0.56329	0.33189	-0.14585	3.6287	0.062822	8.5577

4.2 Numerical Continuation

Truncating $H_{\text{Gauss}}(\epsilon)$ in (4.3) to resolve only N harmonics, we define $H^N_{\text{Gauss}}(\mathbf{a}, \mathbf{b}, \epsilon)$. The associated system of $2N$ Euler-Lagrange equations is

$$\nabla_{\mathbf{a}} H^N_{\text{Gauss}}(\mathbf{a}, \mathbf{b}, \epsilon) = 0, \quad \nabla_{\mathbf{b}} H^N_{\text{Gauss}}(\mathbf{a}, \mathbf{b}, \epsilon) = 0. \tag{4.5}$$

We now seek solutions of the $\epsilon = 0$ system, where all modes are decoupled, that can be continued to $\epsilon = 1$, the desired system. The natural family of solutions is given by (4.4). Thus, for our $\epsilon = 0$ starting point, we consider solutions of the form

$$\mathbf{a}_* = \frac{2^{3/4}}{3\Gamma^{1/2}} (\sigma_1, \sigma_2, \ldots, \sigma_N) \tag{4.6}$$

$$\mathbf{b}_* = \frac{1}{3} \left(1^2, 3^2, \ldots, (2N-1)^2\right) \tag{4.7}$$

where $\sigma_j \in \{-1, 0, 1\}$. The variances, $\mathbf{b}_*$, are unaffected by $\boldsymbol{\sigma}$. Indeed, for $\sigma_j = 0$, b_j is ill-defined, and can take any value.

We now explore continuations from various $\boldsymbol{\sigma}$'s. Before giving the results, we state the conjecture that our computations suggest:

Conjecture 4.1. *For any $N \geq 1$, there is a nontrivial configuration $\boldsymbol{\sigma}$ that can be continued from $\epsilon = 0$ to $\epsilon = 1$. At $\epsilon = 1$, the amplitudes are sign alternating,*

$$\text{sign}(a_p) = (-1)^{(|p|-1)/2}.$$

For a system of two modes ($N = 2$), the numerical continuation of four $\boldsymbol{\sigma}$ configurations is plotted in Figure 1. The configurations $\boldsymbol{\sigma} = (0, 1)$ and $\boldsymbol{\sigma} = (1, -1)$, can be continued to $\epsilon = 1$, while the other two collide and terminate near $\epsilon = 0.368$. Extending this to a system of three modes, we plot the analogous results in Figure 2. Three configurations $\boldsymbol{\sigma} = (0, 1, 0)$, $\boldsymbol{\sigma} = (0, 0, 1)$, and $\boldsymbol{\sigma} = (1, -1, 1)$ can be continued to $\epsilon = 1$. We note that the configurations $\boldsymbol{\sigma} = (0, 1)$, $\boldsymbol{\sigma} = (0, 1, 0)$, and $\boldsymbol{\sigma} = (0, 0, 1)$ are trivial in the sense that they are generated by the reductions of the truncated coupled NLS equations. When more modes are included into the system, these degenerate configurations are destroyed. On the other hand, the configurations $\boldsymbol{\sigma} = (1, -1), (1, -1, 1)$ are non-trivial and persist with respect to adding more modes in the coupled NLS equations. Our results for the non-trivial configurations at $\epsilon = 1$ are summarized in Table 1.

Though computations for two and three modes suggest that an alternating configuration of ± 1's can always be successfully continued to $\epsilon = 1$, this is not the case, as the following

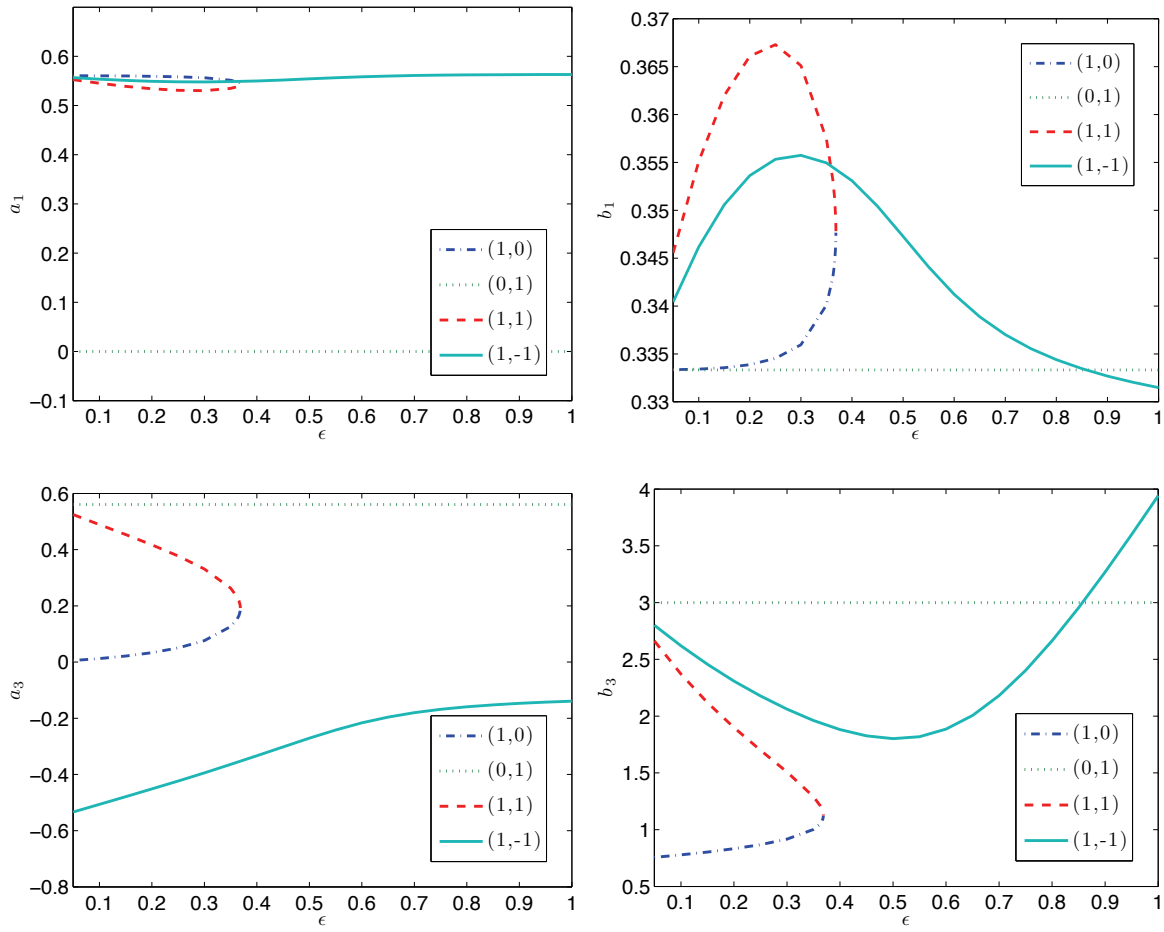

Figure 1: Various continuation branches for a two-mode Rayleigh-Ritz system.

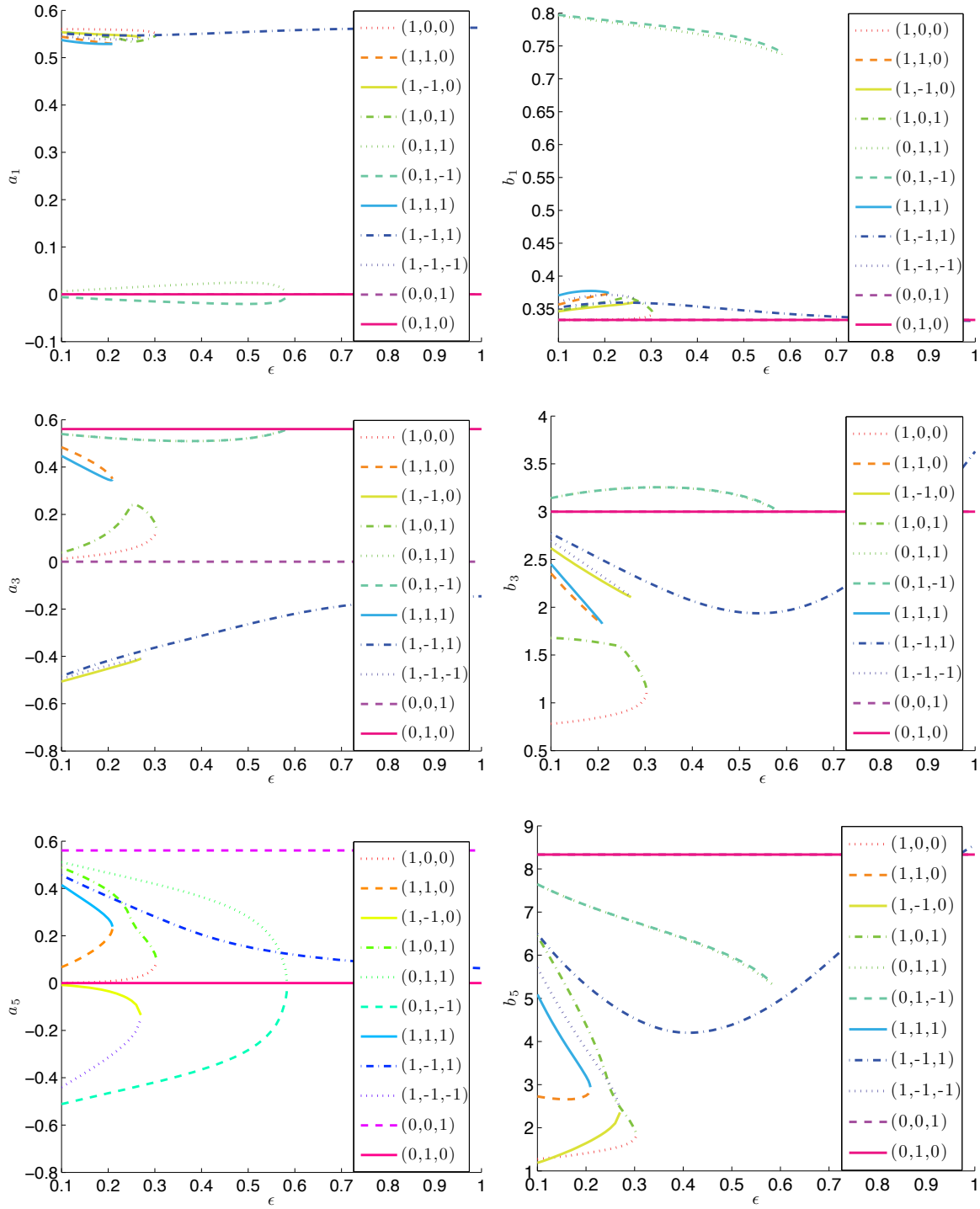

Figure 2: Various continuation branches for a three-mode Rayleigh-Ritz system.

Table 2: Computed values for a truncated Rayleigh-Ritz approximation with fixed $\mathbf{b}_*$ for $\epsilon = 1$. The branch from which we continue is alternating for $1 \leq N \leq 4$: $\boldsymbol{\sigma} = (1), (1,-1), (1,-1,1), (1,-1,1-1)$. The case $N = 5$ is continued from the branch $(1,-1,1,1,1)$ and $N = 6$ is continued from $(1,-1,1,-1,-1,-1)$.

No. of Modes	a_1	a_3	a_5	a_7	a_9	a_{11}
1	0.56060	-	-	-	-	-
2	0.5643	-0.12734	-	-	-	-
3	0.56409	-0.13759	0.061454	-	-	-
4	0.56386	-0.14037	0.068618	-0.037695	-	-
5	0.56372	-0.14139	0.071254	-0.042822	0.026041	-
6	0.56364	-0.14184	0.072457	-0.045015	0.029896	-0.019323

computations demonstrate. We first make the additional simplification, observing that the values of b_j in Table 1 are close to $j^2/3$. This motivates fixing them as such, and only solving the problem for the amplitudes, $\mathbf{a}$. Thus, we solve

$$\nabla_{\mathbf{a}} H^N_{\text{Gauss}}(\mathbf{a}, \mathbf{b}_*, \epsilon) = 0 \tag{4.8}$$

where $\mathbf{b}_*$ is given by (4.7). The results of our computations with these fixed variances are given in Table 2. Continuation from the alternating branch $\boldsymbol{\sigma} = (1,-1), (1,-1,1), \ldots$ is successful till $N = 4$. The alternating branch cannot be continued to $\epsilon = 1$ for five and six modes, though there are other initial states that can be continued to $\epsilon = 1$, with sign sign alternations at $\epsilon = 1$; see Table 2.

Though these results were initially computed using a naive continuation algorithm in MATLAB, solving with a given value of ϵ and using that solution as the initial guess for a larger value of ϵ, they were confirmed by our computations using AUTO [7, 8].

Though the starting branch may not have an alternating sign structure, sign alternating solutions may still be found at $\epsilon = 1$. This makes it challenging to perform numerical continuation with these branches if we no longer assume the variances to be fixed. For a system of five modes, a_7 must change sign. When it crosses zero, the variance becomes ill-defined introducing numerical difficulties. On the other hand, if we iterate the system (4.5) near the solution of (4.8) for $\epsilon = 1$, the convergence is usually achieved with few iterations.

4.3 Tails of the Variational Solutions

Though we are able to construct a sequence of Rayleigh–Ritz approximations with Gaussian ansatz, it is not yet clear if such solutions should exist in space X^s for $s > 1$ or at least have finite power (L^2) in the limit $N \to \infty$. Indeed, the solution $(\mathbf{a}_*, \mathbf{b}_*)$ given by (4.4) for $\epsilon = 0$ with all $a_p \neq 0$ has infinite power, since

$$\sqrt{\tfrac{2}{\pi}} \int_{\mathbb{R}} |a_p \exp(-b_p \zeta^2)|^2 d\zeta = \left(\frac{2}{3}\right)^{3/2} \frac{1}{|p|\Gamma^2}$$

and $\sum_{p\in\mathbb{Z}_{\rm odd}} \frac{1}{|p|} = \infty$. However, the results of Table 2 show that at $\epsilon = 1$, the sign-alternating amplitudes $\{a_p\}_{p\in\mathbb{Z}_{\rm odd}}$ are also decaying in $p \in \mathbb{Z}_{\rm odd}$. We explore whether or not the decay is sufficiently rapid to have finite power and to belong to the energy space, where $H_{\rm Gauss}$ is finite. To this end, we employ a more refined trial-function ansatz, allowing for weak decay of a_p:

$$a_p = A(-1)^{(|p|-1)/2}|p|^{-\gamma}, \quad b_p = \tfrac{p^2}{3}, \quad p \in \mathbb{Z}_{\rm odd} \tag{4.9}$$

where A and γ are unknown parameters to be determined from the Euler-Lagrange equations. If $\gamma > 0$, the Rayleigh-Ritz approximation has both $H_{\rm Gauss}$ and $N_{\rm Gauss}$ finite.

Substituting (4.9) into (4.2) yields a two parameter Hamiltonian

$$h(\gamma, A) = A^2 f(\gamma) - A^4 \Gamma g(\gamma), \tag{4.10}$$

where

$$\begin{aligned} f(\gamma) &= \sum_{p\in\mathbb{Z}_{\rm odd}} \frac{4}{\sqrt{3}}|p|^{-1-2\gamma} \\ g(\gamma) &= \sum_{p,q\in\mathbb{Z}_{\rm odd}} \sqrt{3}\frac{p^{-2\gamma}q^{-2\gamma}}{\sqrt{p^2+q^2}} \\ &\quad + \sum_{p,q,r\in\mathbb{Z}_{\rm odd}} \sqrt{\frac{2}{3}}(-1)^{(|p|+|q|+|r|+|p-q-r|)/2}\frac{|p|^{-\gamma}|q|^{-\gamma}|r|^{-\gamma}|p-q-r|^{-\gamma}}{\sqrt{p^2+q^2+r^2+(p-q-r)^2}} \end{aligned}$$

Solving $\partial_A h(\gamma, A) = 0$, we find

$$A^2(\gamma) = \frac{f(\gamma)}{2\Gamma g(\gamma)}$$

Plugging back in, we get

$$\tilde{h}(\gamma) = h(\gamma, A(\gamma)) = \frac{f(\gamma)^2}{2\Gamma g(\gamma)} - \frac{f(\gamma)^2}{4\Gamma g(\gamma)} = \frac{1}{4\Gamma}\frac{f(\gamma)^2}{g(\gamma)} \tag{4.12}$$

Truncating this approximation to N modes, $\tilde{h}^N(\gamma)$, we are able to identify a sequence of critical points, suggesting convergence as $N \to \infty$ and the existence of a critical point in the primitive functional, (4.12). A few of these approximations are plotted in Figure 3 with $\Gamma = 1$. All of the computed $\tilde{h}^N(\gamma)$'s have the property that

$$\lim_{\gamma\to\infty} \tilde{h}^N(\gamma) = \tilde{h}^1(\gamma) = \frac{8}{9}\sqrt{\frac{2}{3}} \tag{4.13}$$

The critical values of γ, $\gamma_\star$, are given in Table 3. These appear to converge to a value of γ near $\gamma = 1.26$ indicating that the corresponding variational approximations belong to the energy space of the coupled NLS equations. Moreover, since

$$\|U\|_{X^s} \sim \sum_{p\in\mathbb{Z}_{\rm odd}} |p|^{2s-1}|a_p|^2 \sim \sum_{p\in\mathbb{Z}_{\rm odd}} |p|^{2s-1-2\gamma}$$

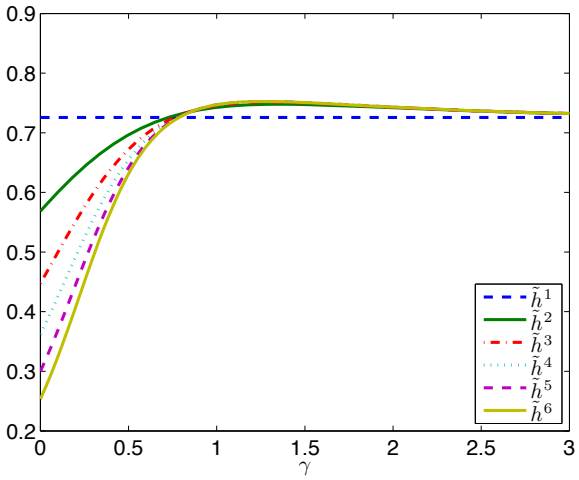

Figure 3: Two–parameter approximation (4.9) of H_{Gauss} for different truncations.

Table 3: Computed critical values of γ for the curves in Figure 3.

No. of Modes	$\gamma_\star$	$\Delta\gamma_\star$
2	1.35511	-
3	1.30184	0.05327
4	1.28176	0.02008
5	1.27208	0.00968
6	1.26672	0.00536

and $\gamma \approx 1.26$, the corresponding variational approximations belong to the space X^s for $s < \gamma$. Therefore, the results of Theorems 1 and 2 can be used in the nonempty interval for the values of $s \in (1, \gamma)$. As it appears that γ is strictly greater than one as the number of modes increases, a solution of infinitely many modes might be more regular than H^1; indeed, it would be Hölder continuous.

The sign alternating structure of the ansatz (4.9) is fundamental for the existence of the critical point of $h(\gamma, A)$. For the variational ansatz,

$$a_p = A|p|^{-\gamma}, \quad b_p = \tfrac{p^2}{3}, \quad p \in \mathbb{Z}_{\text{odd}}, \tag{4.14}$$

we can redo the computations to obtain Figure 4. No critical point of $h(\gamma, A)$ exists for the sign-definite variational approximation (4.14).

5 Numerically Computed Gap Solitons

Using our observations from the Rayleigh-Ritz approximation, we are motivated to solve the xNLS, (3.32), directly for existence of the gap solitons. We note that in [20], the authors explored the related problem of broad band solitons of xNLCME truncated to two modes.

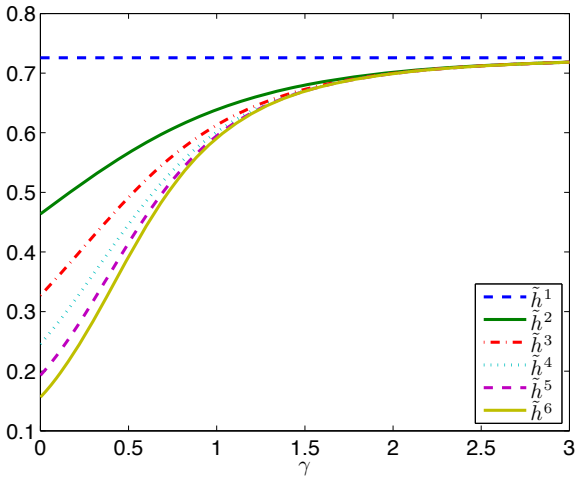

Figure 4: Two–parameter approximation (4.14) of H_{Gauss} for different truncations.

5.1 Computation of the Gap Solitons

We numerically solve equations (3.32) by continuation. Our starting point is the exact solution at $\epsilon = 0$

$$U_p(\zeta; \epsilon = 0) = \tfrac{\sigma_p}{\sqrt{3\Gamma}}\text{sech}(p\zeta),$$

where $\boldsymbol{\sigma}$ is a branch found in Section 4.2 that led to a non-trivial solution at $\epsilon = 1$. Iterating in ϵ, we solve the system (3.32) using MATLAB's `bvp5c` algorithm with absolute tolerance 10^{-4}, relative tolerance 10^{-8}, on the domain $[0, 25]$. `bvp5c` is a nonlinear finite difference algorithm for two-point boundary-value problems discussed in [18]. We use the even symmetry of the solutions to impose the boundary condition $U_p'(0) = 0$, and the artificial boundary condition

$$U_p'(\zeta_{\max}) + pU_p(\zeta_{\max}) = 0.$$

The results for systems of up to six coupled NLS equations at $\epsilon = 1$ appear in Figure 5. As we can see the amplitude decays in p, and they appear to approach some asymptotic profile. We conjecture that this profile persists as additional modes are included. Alternatively, the solution can be expressed as $U(\zeta, \theta)$ by combining the Fourier modes. The resulting solution surface of the integral-differential equation (3.18) appears in Figure 6. The inclusion of additional harmonics induces a more ornate structure near the extrema.

Though we have computed these finite truncation solutions, we reiterate the question whether the corresponding solutions have finite power. For our computed solutions, we find that the power, N_{xNLS}, appears to converge and most of the power remains in the first mode. The data is given in Table 4.

5.2 Gap Solitons in Time Dependent Simulations

Small amplitude gap soliton solutions of the coupled NLS equation (3.17) can be used as initial conditions in the coupled mode equations (1.10) to assess their stability and robustness.

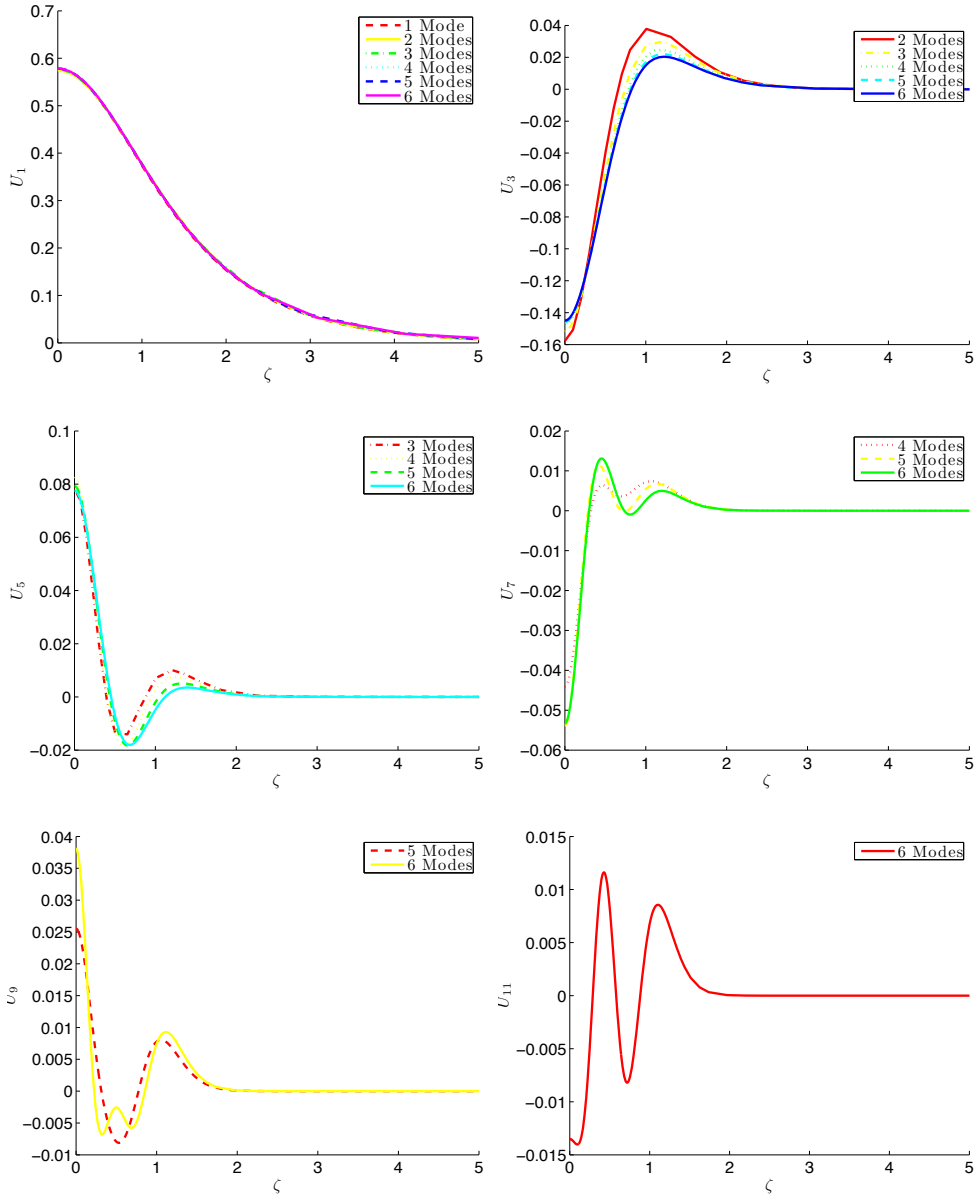

Figure 5: Soliton profiles for the coupled NLS equations (3.17).

Table 4: Computed powers for the soliton profiles appearing in Figure 5.

No. of Modes	$\|U_1\|_{L^2}^2$	$\frac{1}{2}N_{\text{xNLS}}$	$\frac{1}{2}N_{\text{xNLS}} - \|U_1\|_{L^2}^2$
1	0.66667	0.66667	0
2	0.66982	0.68582	0.016000
3	0.67147	0.68929	0.017825
4	0.67211	0.69031	0.018201
5	0.67226	0.69070	0.018441
6	0.67236	0.69088	0.018523

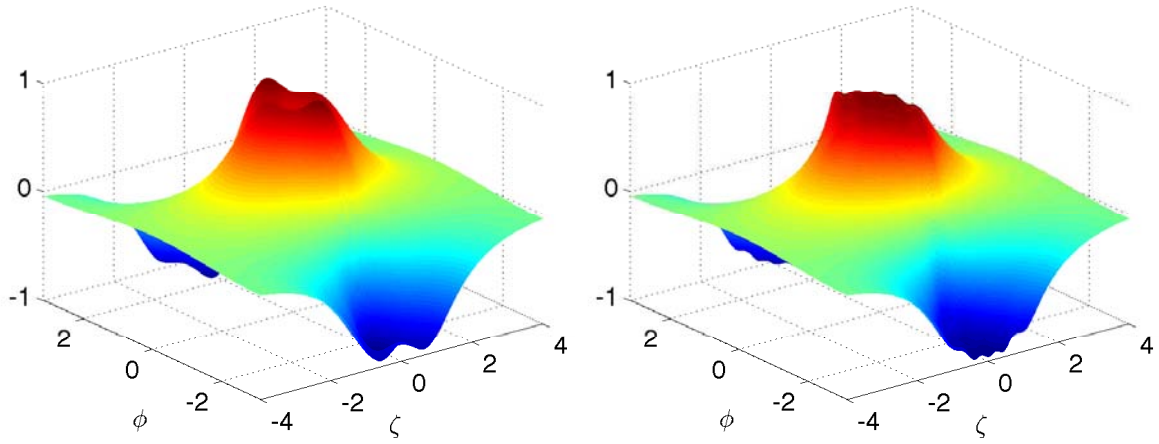

(a) Two Modes (b) Six Modes

Figure 6: The solution surface of the integral-differential equation (3.18) generated by the truncated coupled NLS soliton on Figure 5.

Once the solution $\{U_p(\zeta)\}_{p\in\mathbb{Z}_{\text{odd}}}$ is computed, the initial conditions for the time dependent simulation are given by

$$E_p^+(Z,0) = \mu U_p(\mu Z), \quad E_p^-(Z,0) = -\mu U_p(\mu Z), \quad p \in \mathbb{Z}_{\text{odd}}, \tag{5.1}$$

with even modes set to zero. By Theorem 1, the small amplitude approximation is only accurate up to $\mathcal{O}(\mu^2)$. We explore this small error as a source of the initial perturbation.

We present the results of two and four mode systems. In each case, we truncated both the the system of coupled NLS equations (3.17) and the coupled mode equations (1.10) at the same number of resolved modes. In our simulations, we take as our constants

$$v_g = 1, \quad N_0 = 0, \quad N_{2p} = 1, \quad \Gamma = 1.$$

The simulations were performed with the indicated number of grid points using a pseudo-spectral discretization and RK4 time stepping. For both the two and four mode simulations, the initial conditions (5.1) were computed with greater precision than an in the previous section; the absolute tolerance was 10^{-7} and the relative tolerance was 10^{-9}, and the domain was $[0, 35]$.

In Figure 7, we plot the normalized time-space surfaces of $|E_p^+|$ from our simulations of the first four odd modes. For both values of μ, the solution is persistent, but the oscillations are greater for the larger value of μ, and there is some decoherence near the peak. With the smaller value of μ, there is far less distortion. Additional details of the dynamics are available online in the following animations:

Two Mode Truncation The following simulations were computed with 1024 grid points. The $\mu = .4$ simulations were computed on the domain $[-50, 50]$, the $\mu = .2$ simulations were computed on the domain $[-100, 100]$, and the $\mu = .1$ simulations were computed on the domain $[-200, 200]$.

- http://www.math.toronto.edu/simpson/files/media/broadband/mode1_13.mp4
- http://www.math.toronto.edu/simpson/files/media/broadband/mode3_13.mp4

Four Mode Truncation The following simulations were computed with 2048 grid points. The $\mu = .4$ simulations were computed on the domain $[-50, 50]$, the $\mu = .2$ simulations were computed on the domain $[-100, 100]$, and the $\mu = .1$ simulations were computed on the domain $[-200, 200]$.

- http://www.math.toronto.edu/simpson/files/media/broadband/mode1_1357.mp4
- http://www.math.toronto.edu/simpson/files/media/broadband/mode3_1357.mp4
- http://www.math.toronto.edu/simpson/files/media/broadband/mode5_1357.mp4
- http://www.math.toronto.edu/simpson/files/media/broadband/mode7_1357.mp4

As one would expect, there is better agreement between the approximate small amplitude soliton and the time dependent simulation as $\mu \to 0$. However, for all values of μ presented, there is a persistence of the localization, even if there is distortion to some of the fine structure in the higher harmonics. All of this suggests the gap solutions are robust.

Many other experiments are possible; simulating with more modes, simulating with larger values of μ, and seeding the initial conditions of a smaller system into a larger system. In the previous work [19], the exact gap soliton (3.9) was used as an initial condition for successively larger truncations of the extended coupled mode system (1.10).

6 Open Problems

We conclude this work with a discussion of open problems concerning the existence of non-trivial localized solutions of xNLCME and xNLS, arising for the case of a refractive index composed of an infinite array of Dirac delta functions. Some of the challenges include:

- Prove the existence of a non-trivial critical point to h, (4.10), the single parameter Rayleigh-Ritz approximation,
- Prove the existence of a non-trivial solution to H_{Gauss}, (4.2), the Gaussian Rayleigh-Ritz approximation,
- Prove the existence of a non-trivial solution to the coupled NLS equations (3.17),
- Prove the existence of a non-trivial solution to the coupled mode equations (3.3).

By "non-trivial", we mean a solution in which all modes are active and non-zero. It would also be of interest to obtain proofs of existence for arbitrarily large finite truncations of these problems. Intimately connected with the last two challenges is the question of appropriate function spaces. As discussed in Section 4.3, our variational approximations live in the function space X^s for $1 < s < \gamma \approx 1.26$ for which our Theorems 1 and2 are stated. The upper value on s that ensures that the interval is nonempty is only approximated numerically

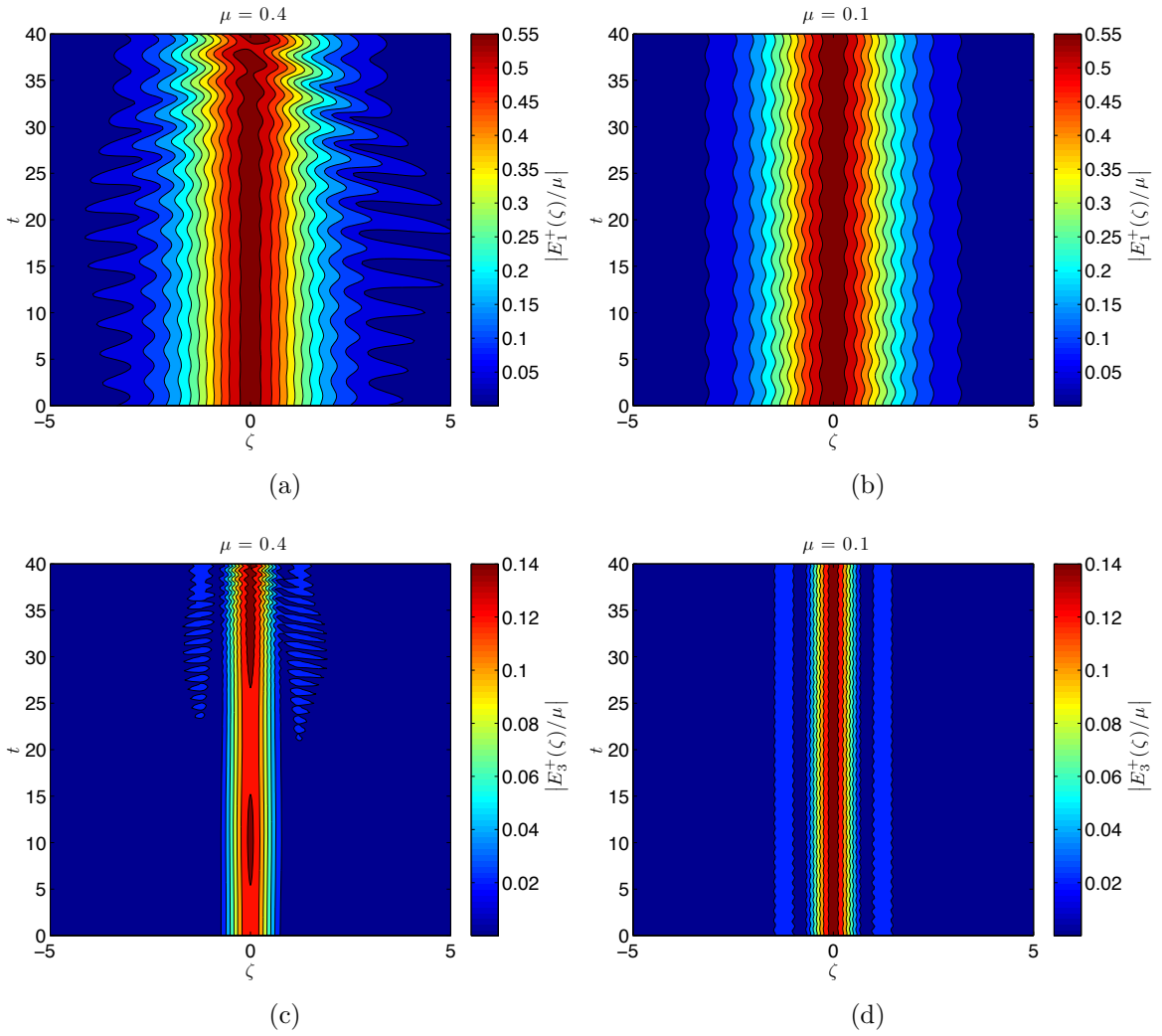

Figure 7: Surfaces generated from simulations of the coupled mode system (1.10) truncated to four modes with initial data (5.1). The $\mu = .4$ simulations were computed on the domain $[-50, 50]$, and the $\mu = .1$ simulations were computed on the domain $[-200, 200]$. In both cases, there were 2048 grid points.

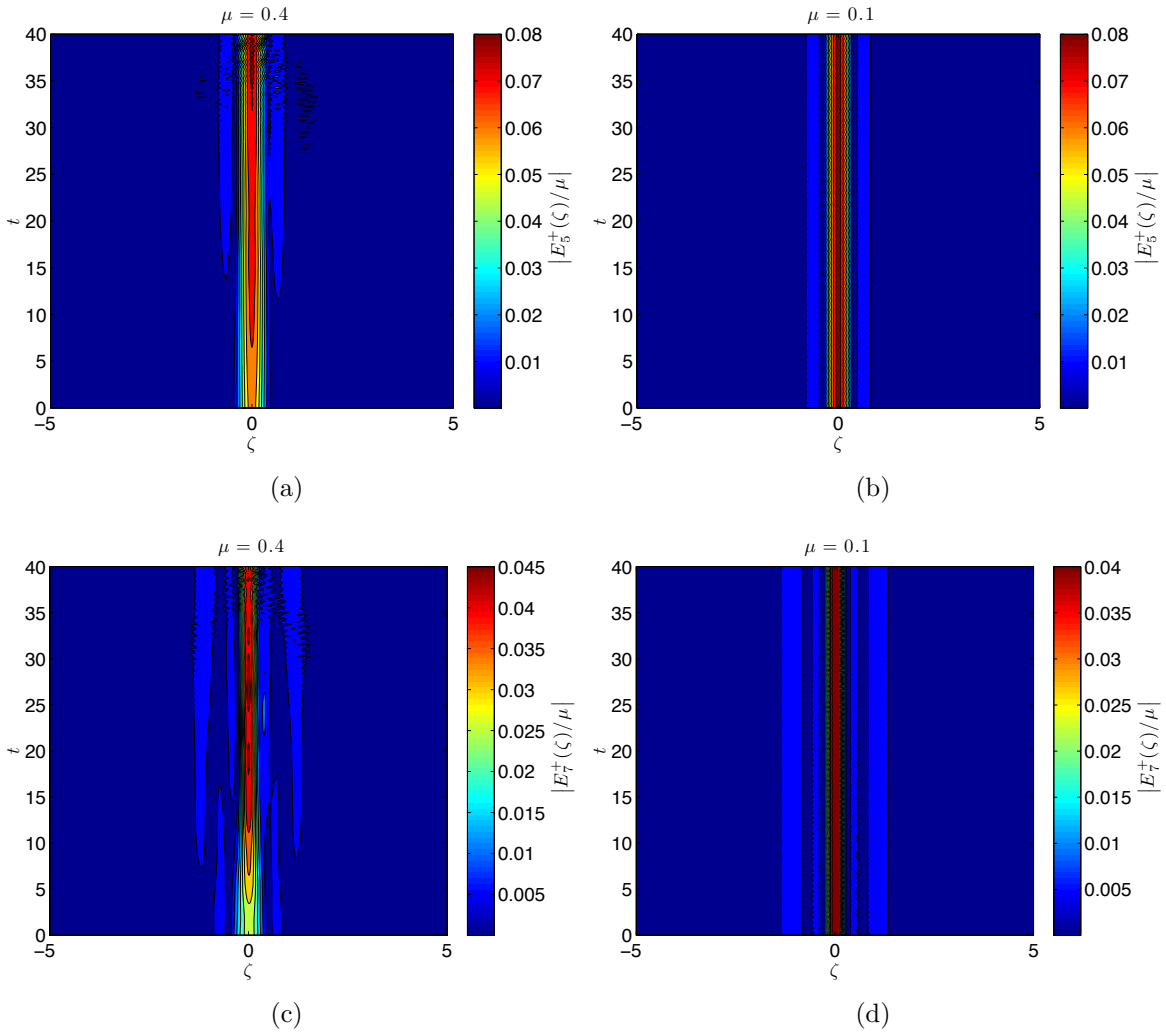

Figure 7 continued.

from the "rough" variational approximation. Of course, it is also possible that such solutions may not exist. A counterexample would also be of interest.

Modeling the nonlinear Maxwell equation with refractive index given by a periodic sequence of Dirac delta-functions is a challenging problem both analytically and numerically. Results of our work give a starting point to further exploration of this system, and the evolution of its localized excitations. The question of localized solutions for xNLCME for less restrictive, and more physical, refractive indices is also of great interest.

References

[1] A. Aceves and S. Wabnitz. Self-induced transparency solitons in nonlinear refractive periodic media. *Physics Letters A*, 141(1-2), 1989.

[2] D. Agueev and D. Pelinovsky. Modeling of wave resonances in low-contrast photonic crystals. *SIAM Journal on Applied Mathematics*, 65(4):1101–1129, 2005.

[3] R. Boyd. *Nonlinear Optics*. Academic Press, 2008.

[4] D. Christodoulides and R. Joseph. Slow bragg solitons in nonlinear periodic structures. *Physical Review Letters*, 62(15):1746–1749, Jan 1989.

[5] M. Chugunova and D. E. Pelinovsky. Block-diagonalization of the symmetric first-order coupled-mode system. *SIAM J. Appl. Dyn. Syst*, 5(1):66–83, 2006.

[6] C. de Sterke and J. Sipe. Gap solitons. *Progress in Optics*, 33:205–205, 1994.

[7] E. Doedel. AUTO: A program for the automatic bifurcation analysis of autonomous systems. *Congressus Numerantium*, 30:265–284, Jan 1981.

[8] E. Doedel, B. Oldeman, and et al. AUTO-07P. `http://indy.cs.concordia.ca/auto/`.

[9] B. Eggleton, C. de Sterke, and R. Slusher. Nonlinear propagation in superstructure bragg gratings. *Optics letters*, 21(16):1223–1225, Jan 1996.

[10] B. Eggleton and R. Slusher. *Nonlinear Photonic Crystals*. Springer, 2010.

[11] R. Goodman, R. Slusher, and M. I. Weinstein. Stopping light on a defect. *Journal of the Optical Society of America B: Optical Physics*, 19(7):1635–1652, Jan 2002.

[12] R. H. Goodman, M. I. Weinstein, and P. Holmes. Nonlinear propagation of light in one-dimensional periodic structures. *Journal of Nonlinear Science*, 11:123–168, 2001.

[13] D. Pelinovsky and G. Schneider. Justification of the coupled-mode approximation for a nonlinear elliptic problem with a periodic potential. *Applicable Analysis*, 86(8):1017–1036, 2007.

[14] D. Pelinovsky and G. Schneider. Moving gap solitons in periodic potentials. *Mathematical Methods in the Applied Sciences*, 31(14):1739–1760, 2008.

[15] J. Ranka, R. Windeler, and A. Stentz. Visible continuum generation in air-silica microstructure optical fibers with anomalous dispersion at 800 nm. *Optics letters*, 25(1):25–27, Jan 2000.

[16] G. Schneider. Nonlinear coupled mode dynamics in hyperbolic and parabolic periodically structured spatially extended systems. *Asymptotic Analysis*, 28(2):163–180, 2001.

[17] G. Schneider and H. Uecker. Existence and stability of modulating pulse solutions in Maxwell's equations describing nonlinear optics. *Zeitschrift für Angewandte Mathematik und Physik (ZAMP)*, 54(4):677–712, 2003.

[18] L. Shampine, I. Gladwell, and S. Thompson. *Solving ODEs with MATLAB*. Cambridge University Press, 2003.

[19] G. Simpson and M. Weinstein. Coherent structures and carrier shocks in the nonlinear maxwell equations. *MMS*, To Appear.

[20] R. Tasgal, Y. Band, and B. Malomed. Gap solitons in a medium with third-harmonic generation. *Physical Review E - Statistical, Nonlinear, and Soft Matter Physics*, 72(1):1–10, Jan 2005.